Type III secretion system of *Pseudomonas aeruginosa* affects mucin gene expression via NF-κB and AKT signaling in human carcinoma epithelial cells and a pneumonia mouse model

Short title: *Pseudomonas aeruginosa* T3SS affects mucin expression

Ji-Won Park[1], In-Sik Shin[2], Sei-Ryang Oh[1], Un-Hwan Ha[3], and Kyung-Seop Ahn[1*]

[1] *Natural Medicine Research Center, Korea Research Institute of Bioscience and Biotechnology, 30 Yeongudanji-ro, Ochang-eup, Cheongwon-gu, Cheongju-si, Chungbuk 28116, Republic of Korea.*

[2] *College of Veterinary Medicine, Chonnam National University, Gwangju, 61188, Republic of Korea*

[3] *Department of Biotechnology and Bioinformatics, Korea University, Sejong 30016, Republic of Korea.*

[*]Author to whom correspondence should be addressed

Kyung-Seop Ahn[a*]

Natural Medicine Research Center,

Korea Research Institute of Bioscience and Biotechnology,

30 Yeongudanji-ro, Ochang-eup, Cheongwon-gu, Cheongju-si, Chungbuk 28116, Republic of Korea.

Tel: +82-43-240-6113; Fax: +82-43-240-6129

E-mail: ksahn@kribb.re.kr

Abstract

The type III secretion system (T3SS) in *Pseudomonas aeruginosa* has been linked to severe disease and poor clinical outcomes in animal and human studies. Of the various T3SS effector genes, ExoS and ExoT showed mutually exclusive distributions, and these two genes showed varied virulence. We aimed to investigate whether the ExoS and ExoT effector proteins of *P. aeruginosa* affect the expression of the proinflammatory mediators Muc7, Muc13, Muc15, and Muc19 via the NF-κB and AKT signaling pathways. To understand the role of the T3SS, we used ΔExoS, ΔExoT, and T3SS transcriptional activator ExsA mutants (ExsA::Ω), as well as A549 cells stimulated with *P. aeruginosa* strain K (PAK). We investigated the effects of ΔExoS, ΔExoT, and ExsA::Ω on the development of pneumonia in a mouse model and on Muc7, Muc13, Muc15, and Muc19 production in A549 cells. ΔExoS and ΔExoT markedly decreased the neutrophil count in the bronchoalveolar lavage fluid, with a reduction in Muc7, Muc13, Muc15, and Muc19 expression. ΔExoS and ΔExoT reduced NF-κB and AKT phosphorylation, together with Muc7, Muc13, Muc15, and Muc19 expression in PAK-infected mice and A549 cells. In conclusion, *P. aeruginosa* infection induced the expression of Mucus, and the *P. aeruginosa* T3SS appeared to be a key player in Muc7, Muc13, Muc15, and Muc19 expression, which is further controlled by NF-κB and AKT signaling. These findings might be useful to devise a novel therapeutic approach for the treatment of chronic pulmonary infections by targeting ExoS and ExoT.

45 **Author Summary**

46 *Pseudomonas aeruginosa* is a ubiquitous gram-negative bacterium causing serious infections.
47 Many clinical isolates of *P. aeruginosa* have a specialized apparatus for injecting toxins into
48 eukaryotic cells, namely, the type III secretion system (T3SS). The T3SS is a syringe-like
49 apparatus on the bacterial surface, with 4 effector toxins: ExoS, ExoT, ExoY, and ExoU. We
50 investigated the effect of ExoS and ExoT of the T3SS of *P. aeruginosa* K strain (PAK). Mucus
51 plays a vital role in protecting the lungs from environmental factors, but conversely, in muco-
52 obstructive airway disease, mucus becomes pathologic. We showed that infection with ExoS
53 and ExoT induced Muc7, Muc13, Muc15, and Muc19 expression in host cells. PAK clinical
54 strains induce proinflammatory cytokine production through the T3SS, and this involves NF-
55 κB and SP1/AKT activation in pneumonia mouse models. Mucus induction in response to
56 ExoS and ExoT infection relied on NF-κB and SP1/AKT activation. Our findings highlight the
57 roles of Muc7, Muc13, Muc15, and Muc19 in inducing proinflammatory cytokine expression
58 during ExoS and ExoT exposure in PAK infections, paving the way for a novel therapeutic
59 approach for the treatment of pulmonary infections.

60

Introduction

The gram-negative bacterium *Pseudomonas aeruginosa* uses a complex type III secretion system (T3SS) to inject effector proteins into host cells [1,2]. The T3SS is a major virulence determinant that manipulates eukaryotic host cell responses that is present in a broad range of pathogens. It is a specialized needle-like structure that delivers effector toxins directly from the bacterium into the host cytosol in a highly regulated manner [3]. This system is activated on contact with eukaryotic cell membranes, interferes with signal transduction, and causes cell death or alterations in host immune responses [4]. The T3SS in *P. aeruginosa* has been linked to severe disease and poor clinical outcomes in animal and human studies [4,5]. The features of this interesting secretion system have important implications for the pathogenesis of *P. aeruginosa* infections and for other T3SSs. *P. aeruginosa* has four known effector toxins: ExoS, ExoT, ExoY, and ExoU. These proteins can modify signal transduction pathways and counteract innate immunity [6,7]

Mucins are a major component of the respiratory mucus. Mucins are either membrane-bound (like MUC1) with a role in sensing external information and transducing it to cells, or secreted, the type of which is characterized by a high molecular weight and viscosity. They are glycoproteins secreted by the mucosal and submucosal glands. The mucin molecule consists of a polypeptide core with branched oligosaccharide side chains, each of which contains 8 to 10 sugars [8,9]. Molecular cross-linking of this structure contributes to the viscoelastic property of mucus [10]. Despite their recalcitrance, mucins are a main nutrient source for niche-specific microbiota of the gut and oral cavity. For example, oral streptococci produce a variety of glycolytic and proteolytic enzymes that liberate bioavailable carbohydrates from salivary glycoproteins [11,12]. At least 20 human mucin genes have been identified by cDNA cloning:

84 *MUC1*, *MUC2*, *MUC3A*, *MUC3B*, *MUC4*, *MUC5AC*, *MUC5B*, *MUC6*, *MUC7*, *MUC8, MUC9,*
85 *MUC12*, *MUC13*, *MUC15*, *MUC16*, *MUC17*, *MUC19*, *MUC20*, *MUC21*, and *MUC22*) [13].
86 However, these mucins cannot maintain homeostasis in intrabronchial respiratory epithelial
87 cells of patients with weak immunity, and when overexpressed, cause mucous membrane
88 damage due to excessive secretion of mucus, and need to be blocked. However, the underlying
89 mechanisms have been clearly clarified for only a few mucins to date. Muc7, Muc13, Muc15,
90 and Muc19 have been implicated in bronchial inflammation among mucin targets, but the
91 mechanism of the mechanism has not been studied to date. Especially in immunocompromised
92 patients and children infected with the opportunistic pathogen *P. aeruginosa*, the risk of
93 secondary infection is high and leads to not only asthma and airway hypersensitivity as well as
94 deterioration of existing disease, but also mucus accumulation, which can result in terrible
95 death due to difficulty of breathing by chronic obstructive pulmonary disease [14,15]. However,
96 the mechanism underlying this condition is yet to be clarified.

97 NF-κB is also a high expression level transcription factor involved in many
98 inflammation`s formation and development [16]. Moreover, SP1/NF-κB pathway has been
99 reported connected to cell migration, invasion and EMT (epithelial to mesenchymal transition)
100 recently [17,18]. Furthermore, SP1 and NF-κB (p65) were found significantly upregulated in
101 ExoS and ExoT infected cell. The ExsA::Ω and ΔST does not increased the expression level
102 of SP1 and NF-κB (p65) in vitro and in vivo. The expression level of Muc7, Muc13, Muc15,
103 and Muc19 may be increased through activation of SP1 and NF-κB (p65) due to infection of
104 ExoS and ExoT.

105 Here, we investigated the effect of ExoS and ExoT of *P. aeruginosa* strain K (PAK) on
106 the induction of Muc7, Muc13, Muc15, and Muc19 expression, as well as the underlying

mechanism, in host cells and a pneumonia mouse model. We expected our study to provide new insights into the roles of Muc7, Muc13, Muc15, and Muc19 in inducing proinflammatory cytokine expression in response to ExoS and ExoT exposure in PAK infection.

Materials and Methods

Bacterial strains

All strains and plasmids used in this study are listed in Supporting information S1 Table. Chromosomal mutants were all derived from the same parental PAK strain, as indicated in S1 Table, and were generated by allelic exchange (for details, see the Supporting information S1 Text). PAK strains vary widely in their expression of virulence genes. The strain used in this study strongly expresses the T3SS genes. Regions flanking the appropriate mutation were amplified using chromosomal DNA as a template (unless specified otherwise), joined by "splicing by overlap extension PCR," and cloned into the appropriate plasmid using the indicated restriction enzymes. PAK-ΔST is a *P. aeruginosa* clinical isolate that naturally carries the ExoY gene, but lacks the genes for ExoS and ExoT. We reported that the pUCP18-PAKexoS (S) and pUCP18-PAKexoT (T) mutant strains are secretion competent and export the expected effector proteins [19]. Antibiotics were used when necessary at the following concentrations: for plasmids in *Escherichia coli*, 50 μg/mL ampicillin, 15 μg/mL gentamicin, and 25 μg/mL kanamycin; for *P. aeruginosa*, 500 μg/mL carbenicillin, 100 μg/mL gentamicin, and 100 μg/mL tetracycline.

Human cell culture

A549 adenocarcinomic human alveolar basal epithelial cells, and H292 human airway epithelial cells were purchased from the American Type Culture Collection (ATCC, Manassas, VA, USA). The cells were maintained in RPMI1640 (Invitrogen, Grand Island, NY, USA) supplemented with 10% fetal bovine serum (FBS; Invitrogen) in the presence of penicillin (100 U/mL), streptomycin (100 μg/mL; Sigma-Aldrich, St. Louis, MO, USA), and HEPES (25 mM),

133 at 37 °C in a 5% CO_2 atmosphere.

134

135 ***In-vitro* bacterial infection**

136 For direct bacterial challenge of A549 cells, bacterial strains were grown in tryptic soy
137 broth (Sigma-Aldrich) at 37 ° C until the OD_{600} reached 1. The bacterial cultures were
138 centrifuged at 7,000 × *g* for 10 min, washed with PBS, and resuspended at a ratio of 1:20
139 bacterial cells to A549 cells or H292 cells.

140

141 **qRT-PCR analysis**

142 Total RNA was extracted using TRIzol® reagent (Invitrogen) following the
143 manufacturer's protocol and was used to synthesize cDNA using the AMPIGENE® cDNA
144 Synthesis Kit (Enzo Life Sciences, NY, USA). PCRs were conducted using SYBR Green PCR
145 Master Mix (KAPA Biosystems, Woburn, MA, USA) and the primers listed in S2 Table.
146 Reactions were run in a CFX96 real-time PCR system (Bio-Rad, Hercules, CA, USA) using
147 the following thermal conditions: stage 1, 50°C for 2 min and 95°C for 10 min; stage 2, 95°C
148 for 15 s and 60°C for 1 min. stage 2 was repeated for 40 cycles. Relative mRNA levels were
149 calculated using the comparative CT method and normalized to the level of GAPDH.

150

151 **Immunoblot analysis**

152 Cells were lysed with 20 mM Tris-HCl (pH 7.4), 50 mM NaCl, 50 mM sodium
153 phosphate, 30 mM NaF, 5 μM zinc chloride, 2 mM iodoacetic acid, and 1% Triton X-100 for
154 10 min at room temperature on ice for 20 min with regular vortexing. The lysate was
155 centrifuged at 16,000 × *g* for 10 min at 4 ° C and the supernatant was collected. The protein

concentration in the supernatant was measured using bicinchoninic acid (Pierce, Rockford, IL, USA). Proteins were separated by SDS-PAGE and transferred to polyvinylidene difluoride membranes.

Membranes were blocked in TBS (10 mM Tris-HCl (pH 7.5), 150 mM NaCl) containing 5% nonfat dry milk for 2 h and incubated with the primary antibodies anti-Muc7 (Enzo Life Sciences, Farmingdale, NY, USA), anti-Muc13 (Thermo-Fisher Scientific, Waltham, MA, USA), anti-Muc15 (Enzo Life Sciences, Farmingdale, NY, USA), anti-Muc19 (Enzo Life Sciences), anti-p65 (Santa Cruz, Dallas, TX, USA), anti-phospho-p65 (Cell Signaling, Danvers, MA, USA), anti-IκBα (Cell Signaling), anti-phospho-IκBα (Cell Signaling), anti-AKT (Cell Signaling,), anti-phospho AKT (Cell Signaling), anti-SP1 (Santa Cruz) or β-actin (Thermo-Fisher Scientific) for 18 h at 4 °C. The immunoblots were washed and incubated with appropriate secondary antibodies and visualized using SuperSignal™ West Pico Chemiluminescent Substrate (Pierce, Rockford, IL, USA) or SuperSignal™ West Femto Maximum Sensitivity Substrate (Pierce).

Promoter analysis

SP1 promoter activity was assessed using a luciferase assay system (Promega, Madison, WI, USA) according to the manufacturer's instructions, and β-galactosidase expression (pCH110) was used for normalization. A549 cells were transfected with pGL4.14 and the indicated luciferase SP1 promoter construct.

A549 cells were transfected with pGL4.43 (luc2P/NF-κB-RE/Hygro) plasmid using Lipofectamine 2000 transfection reagent (Invitrogen/Thermo-Fisher Scientific, Carlsbad, CA, USA) according to the manufacturer's protocol. Twenty hours after transfection, the cells were

179 stimulated with PAK for 2 h, harvested, and assessed for luciferase activity using the ONE-
180 Glo™ luciferase reporter assay system (Promega) according to the manufacturer's instructions.
181
182 **Immunohistochemistry**
183 H292 cells were cultured on Permanox plastic chamber slides (Nunc, Rochester, NY,
184 USA) and fixed in methanol at 4°C for 20 min. The slides were washed three times with PBS,
185 and blocked with 3% (w/v) BSA in PBS for 30 min. Then, the slides were incubated with anti-
186 NF-κB p65 subunit (rabbit polyclonal IgG, 1:200 dilution, Santa Cruz) antibody at 4°C for 24
187 h. The slides were washed to remove excess primary antibody and then incubated with anti-
188 rabbit Alexa Fluor 488-conjugated secondary antibody (Invitrogen, Carlsbad, CA) for 2 h at
189 room temperature, washed with PBS, and then mounted using ProLong Gold Antifade reagent
190 containing 4',6-diamidino-2-phenylindole (DAPI) (Invitrogen) for 5 min prior to visualization
191 by confocal laser scanning microscopy (LSM510; Carl Zeiss, Oberkochen, Germany). All
192 samples were photographed under the same exposure conditions, and nuclei were quantified
193 from the images obtained.
194
195 **Animal infection**
196 Four-week-old, specific pathogen-free female C57BL/6 mice were purchased from the Orient
197 Co. (Seoul, Korea) and were used after a week of quarantine and acclimatization. The mice
198 were allowed access to sterilized tap water and standard rodent chow. Bacteria were
199 centrifuged and resuspended to the appropriate CFU/mL in PBS as determined by optical
200 density, and plated out in a serial dilution on nutrient broth agar plates. LPS was injected
201 intranasally by dissolving 5 μg in 50 μl of PBS. Mice were slightly anaesthetized by

intraperitoneal injection of pentobarbital (Virbac, Fort Worth, TX, USA). Bacterial solutions at appropriate concentration (2.5×10^6 CFU per mouse in 50 µL PBS) were then administered by intranasal instillation (25 µL per nostril). Control mice were inoculated intranasally with 50 µL of PBS. Survival experiments and analysis of bronchoalveolar lavage fluid (BALF) were performed as previously described [20,21]

Histology

After BALF samples were obtained, the mice were sacrificed by intraperitoneal injection of pentobarbital (50 mg/kg; Hanlim Pharm. Co., Seoul, Korea), and lung tissues were collected and fixed in 10% (v/v) neutral-buffered formalin. The tissues were embedded in paraffin, sectioned at 4-µm thickness, and stained with hematoxylin and eosin solution (hematoxylin, Sigma MHS-16; eosin, Sigma HT110-1-32). Quantitative analysis of inflammation and mucus production was performed in at least 4 squares per slide using an image analyzer (Molecular Devices Inc., Sunnyvale, CA, USA).

siRNA-mediated knockdown

siRNAs targeting IKKα and IKKβ were designed and synthesized by Dharmacon (Lafayette, CO, USA). A549 cells were resuspended in serum-free DMEM, and 2.5×10^5 cells/mL were seeded in a 12-well plate and transfected with siRNA-IKKα/siRNA-IKKβ or siRNA-negative control (NC), using Lipofectamine RNAiMAX (Invitrogen; Thermo Fisher Scientific, Inc.). After 6 h, the medium was changed with RPMI1640 containing 10% FBS. Cells were harvested at 48 h after transfection for RT-qPCR or at 72 h for western blot analysis. Three different IKKα/IKKβ-specific siRNAs were screened, and the most efficient one was

225 selected for experiments.

226

227 **Ethics Statement**

228 All experimental procedures were carried out in accordance with the NIH Guidelines for the
229 Care and Use of Laboratory Animals and were approved by the Korea Institute of Bioscience
230 and Biotechnology Animal Care and Use Committee (IACUC KRIBB-AEC-14094).

231

232 **Statistical analysis**

233 Data represent the mean ± standard error of the mean (SD). Statistical differences
234 among groups were determined by one-way ANOVA with repeated measures followed by
235 Newman–Keuls testing in SPSS 14.0 (IBM Software, Armonk, NY, USA). $P < 0.05$ was
236 considered statistically significant.

Results

Muc7, Muc13, Muc15, and Muc19 expression is increased in PAK-infected A549 and H292 cells

P. aeruginosa PAK affected the expression of Muc7, Muc13, Muc15, and Muc19 in a MOI-and time-dependent manner. As the multiplicity of infection (MOI) of PAK increased, the expression of Muc7, Muc13, Muc15, and Muc19 in A549 cells increased at the mRNA (Fig 1A–D) and the protein (Fig 1I) level. The mRNA expression of all 4 mucins tended to decrease after 12 h, while at the protein level, expression decreased after 4 h (Fig 1E–H, J). Immunohistochemistry (IHC) of H292 cells infected with PAK at MOI 20 confirmed the increase in Muc7, Muc13, Muc15, and Muc19 (Fig 1K). Thus, Muc7, Muc13, Muc15, and Muc19 in A549 cells increased in a concentration- and time-dependent manner by PAK infection.

Effects of NF-κB signaling inhibitors BAY11-7082 and LY-294002 on Muc7, Muc13, Muc15, and Muc19 expression and NF-κB p65 and AKT phosphorylation in PAK-infected A549 cells

Bay11-7082 is an IκBα inhibitor and LY-294002 is a well-known inhibitor of PI3K signaling. We previously reported that PAK increased p65 phosphorylation in an epithelial cell line [22]. In addition, PAK reportedly increased AKT phosphorylation lung cancer cells [23,24]. Therefore, we tested the effects of the above inhibitors on mucin expression in A549 cells infected by PAK. Bay11-7082 and LY-294002 suppressed the increases in Muc7, Muc13, Muc15, and Muc19 mRNA expression induced by PAK (Fig 2A–D). The effect of PAK on Muc7 expression was hardly affected by the inhibitors while Muc13 expression was less

affected. Muc15 and Muc19 were more strongly suppressed in the presence of LY-294002 than in the presence of Bay11-7082. Similar findings were obtained for protein expression by western blotting (Fig 2E).

Phosphorylation of NF-κB and AKT was assessed in PAK-infected A549 cells in the presence or absence of each inhibitor. In PAK-infected A549 cells, luciferase assay indicated that transcription factor activities of NF-κB and SP1 increased. In the presence of Bay11-7082 and LY-294002 these PAK-induced transcription factor activities of NF-κB and SP1 were significantly suppressed as indicated by luciferase analysis and western blot analysis (S1A–D Fig). In PAK-infected A549 cells, the proinflammatory cytokines IL-8 and IL-6 increased, while Bay11-7082 and/or LY294002 significantly suppressed this response as indicated by qRT-PCR and ELISA of IL-6 and IL-8 (S2A–D Fig). Thus, PAK-induced NF-κB and SP1 signal transduction as well as IL-8 and IL-6 of proinflammatory cytokine expression is suppressed by the use of the inhibitors BAY11-7082 and LY-294002 in A549 cells.

ExsA::Ω mutant does not induce expression of Muc7, Muc13, Muc15, and Muc19 via NF-κB p65 and AKT phosphorylation in PAK-infected A549 cells

ExsA::Ω is a mutant that has no functional T3SS. We compared the induction of expression of the 4 mucins in A549 cells between PAK and exsA::Ω. As expected, mRNA expression of all 4 mucins was significantly induced by wild-type PAK, while exsA::Ω did not induce their expression as compared to non-infected control cells (Fig 3A–D). Similar findings were obtained for mucin protein expression (Fig 3A–D). AKT and SP1 phosphorylation was less strongly induced by exsA::Ω than by wild-type PAC as indicated by western blotting (Fig 3E). SP1 and NF-κB transcription factor activities were significantly induced by wild-type

283 PAC but not by exsA::Ω as indicated by luciferase assays (Fig 3F, H). Similar to AKT and SP1
284 phosphorylation, p65 and IκBa phosphorylation was less strongly induced by exsA::Ω than by
285 wild-type PAC as indicated by western blotting (Fig 3I). IHC confirmed the findings for SP1
286 and p65 (Fig 3G, J). There are multiple reports that PAK affects NF-κB signaling, but there
287 was no report that PAK phosphorylated p65, IκBa and SP1 to affect Muc7, Muc13, Muc15,
288 and Muc19 in experiments using A549 cells.. Taken together, these results indicated that a
289 functional T3SS is required for PAK to exert its effects on SP1/AKT signaling, NF-κB
290 signaling, and mucin gene expression.
291
292
293 **ExoS and ExoT of T3SS are required for the increase in Muc7, Muc13, Muc15, and**
294 **Muc19 and inflammatory cytokine expression in A549 cells**
295 Next, we assessed the roles of ExoS and ExoT in the induction of mucin expression
296 by using a mutant strain defective in these two proteins (ΔST) and complementation strains of
297 ΔST with either of the proteins restored (S, expressing ExoS only, and T, expressing ExoT
298 only). We observed that ExoS and ExoT are critical for the expression of the 4 mucins gene in
299 A549 cells as ΔST could not induce Muc7, Muc13, Muc15, and Muc19 expression, while the
300 induction of mucin expression was partially restored in the complementation strains restored
301 their expression induction. Real-time PCR and ELISA indicated that IL-6 expression was
302 restored to approximately 90% and 80% of the PAK-induced level in case of infection with
303 ExoS and ExoT, respectively, and TNF-α was restored to about 60% and 55% of the PAK-
304 induced level in case of infection with ExoS and ExoT, respectively (S3A–D Fig). Thus, in
305 accordance with previous reports, the expression of Muc7, Muc13, Muc15, and Muc19 and

306 proinflammatory cytokines induced by PAK in A549 cells, requires ExoS and ExoT. In cells
307 treated with ExsA::Ω, the increase in IL-6 and TNF-α was suppressed as compared to cells
308 treated with wild-type PAK. ΔST totally lost the ability to induce IL-6 and TNF-α, while this
309 ability was restored in the complementation strains expressing either ExoS (S) or ExoT (T)
310 (S3A–D Fig).
311
312 **ExoS and ExoT of T3SS are required for the increase in Muc7, Muc13, Muc15, and**
313 **Muc19 expression via NF-κB p65 and AKT phosphorylation in A549 cells**
314 Next, we investigated whether ExoS and ExoT are related to known SP1/AKT and
315 NF-κB signals, which are involved in pneumonia and lung diseases, using the mutant strains.
316 The results showed that S and T induced the activation of the SP1/AKT pathway and AKT and
317 p65 phosphorylation in A549 cells nearly to the level the wild-type PAK strain did, while ΔST
318 completely the ability to do so (Fig 5A–D). In particular, it was confirmed that increased SP1,
319 known as a transcription factor for AKT and increases the phosphorylation of IκBα (Fig. 5A–
320 D). These results indicated that ExoS and ExoT are important virulence factors of *P.*
321 *aeruginosa* and are very important for the induction of the inflammatory response in host cells.
322
323 **Effect of PAK infection in a pneumonia mouse model and the roles of ExoS and ExoT**
324 **therein**
325 We determined the PAK infection level in a C57BL/6 mouse model. It is known that
326 PAK infection at specific MOI induces an inflammatory in mice. Accordingly, we tested PAK
327 infection at different MOIs to select the most appropriate one. Pure LPS was used as a control,
328 and mice were subjected to infection with PAK alone (PAK) or together with LPS treatment

329 (PAK+LPS). PAK or LPS was diluted with PBS to inject into mice. Experiments were
330 conducted using 7-8 mice per group. The protein levels of Muc13, Muc15, and Muc19 were
331 increased in lung tissues of PAK+LPS-infected mice (S4A–C Fig). Hematoxylin and eosin
332 (H&E) staining of lung tissues revealed that inflammatory cells were increased in PAK-
333 infected and in PAK+LPS-treated mice. In particular, treatment of PAK+LPS together with
334 LPS and PAK alone resulted in a much greater increase in inflammatory cells. (S5 Fig).
335 When we tested the ΔST, S, and T strains, Muc7, Muc13, Muc15, and Muc19 mRNA
336 and protein expression were significantly increased by S and T, but not ΔST, as indicated by
337 qPCR and western blotting (Fig 6A–E). Similar findings were achieved for proinflammatory
338 cytokine expression (data not shown). Thus, mucin gene expression in the mouse lungs in
339 response to *P. aeruginosa* infection is controlled by ExoS and ExoT.
340
341 **Roles of ExoS and ExoT in AKT activation in mice**
342 Proinflammatory cytokine production was increased through the T3SS of PAK, and
343 this involves AKT activation in pneumonia mouse models. To confirm the role of SP1 in S-
344 and T-infected pneumonia model mice, we evaluated the level of AKT phosphorylation by
345 western blot analysis using antibodies to SP1, AKT, and pAKT. Non-treated as well as ΔST-
346 treated cells displayed weak AKT phosphorylation, whereas S- and T-treated monolayers
347 showed a significant increase in SP1 translocation, which was detectable as of 30 min and was
348 sustained for 1 h (Fig 7A).
349
350 **IKK-α and IKK-β are necessary for NF-κB phosphorylation in response to S and T**
351 **infection**

352 The IκB kinase enzyme complex is part of the upstream NF-κB signal transduction
353 cascade. The IκB kinase (IKK) is an enzyme complex that is involved in propagating the
354 cellular response to inflammation [25]. Small interfering (si)RNA is one of the experimental
355 tools for functional analyses. We used siRNAs to knock out IKKα and IKKβ expression. The
356 presence of control siRNA (siNC) did not affect the increase in muc7, Muc13, Muc15, and
357 Muc19 expression induced in A549 cells by PAK infection. However, knockout of IKKα and
358 IKKβ suppressed the increases in muc7, Muc13, Muc15, and Muc19 by 50% (S6A–D Fig).
359 ELISA of proinflammatory cytokines IL-6 and IL-8 revealed similar effects as those observed
360 for the mucins (S7A, B Fig).

361 Next, we conducted experiments using the strains S and T. A549 cells infected with
362 PAK, ExoS, or ExoT after siNC transfection induced increased muc7, Muc13, Muc15, and
363 Muc19 expression as compared to the negative control. However, in A549 cells infected with
364 PAK, ExoS, or ExoT after knockout of IKKα and IKKβ, the increases in Muc7, Muc13, Muc15,
365 and Muc19 were suppressed by 40–60% (Fig 8A–D).

Discussion

T3SS gene expression is induced by contact with eukaryotic cells or under specific environmental conditions [26]. ExoS and ExoT are toxins with adenosine diphosphate ribosyltransferase and Rho guanosine triphosphatase activities [27]. They are similar in structure, but the toxicity of ExoT is less potent than that of ExoS [28,29]. When activated, these proteins destroy the actin filaments that make up the cytoskeleton of the host, thus inhibiting phagocytosis and finally killing the host cell [30]. We found that S and T complementation strains were extremely efficient in lysing eukaryotic cells, and this observation corresponded with their highly toxic phenotypes in a pneumonia mouse model. S and T were found to be as damaging as the T3SS-proficient PAK strain in mice. Histological analysis *in vivo* showed that S- and T-infected lungs had damage lesions.

P. aeruginosa ExoS and ExoT were suggested to be associated with lung injury and mucus accumulation in mice [31,32], but these types of virulence mechanisms have never been investigated at the molecular level. The way in which these major virulence determinants of *P. aeruginosa* function to cause severe disease during infection was not clear until date. Therefore, the effects of NF-κB and SP1/AKT activities on the expression of Muc7, Muc13, Muc15, and Muc19 in S- and T-infected pneumonia model mice were investigated. Expression and delivery of Muc7, Muc13, Muc15, and Muc19 were found to be improved by S and T infection. Examination of infected A549 cells revealed that the expression of Muc7, Muc13, Muc15, and Muc19 is dependent on NF-κBp65 and SP1/AKT phosphorylation. In particular, overexpression of the inflammatory cytokines (IL-6, IL-1β, and TNF-α) in response to activation of ExoS- and ExoT-induced NF-κB and AKT was associated with the pathogenesis mechanism in the pneumonia mouse model. In addition, proinflammatory cytokine expression

389 as well as expression of Muc7, Muc13, Muc15, and Muc19 was increased upon infection with
390 strains S and T. Our results suggest that ExoS and ExoT play important roles in the genetic
391 etiology associated with acute and chronic infections.

392 *P. aeruginosa* is known to have an important influence on the activation of NF-κB and
393 SP1 in pulmonary diseases and to regulate the production of cytokines, matrix
394 metalloproteinases (MMPs), and mucins [4,33]. Muc7, Muc13, Muc15, and Muc19 gene and
395 protein expression is facilitated by several cytokines, including TNF-α and IL-1β, secreted by
396 macrophages [8,34]. In previous reported that IL-6, IL-8, and TNF-α secreted by lung
397 lymphocytes specifically induce the secretion of Muc7, Muc13, Muc15, and Muc19 to promote
398 destruction of lung tissue [35,36]. Muc7, Muc13, Muc15, and Muc19, IL-1β, and TNF-α
399 expression levels in response to infection were significantly reduced in A549 cells transformed
400 with siRNA targeting IKK-α and IKK-β. This shows that Muc7, Muc13, Muc15, and Muc19
401 are required for the expression of proinflammatory cytokines. Since mucin expression is known
402 to increase respiratory irritation in pulmonary infections, it further implies cytokine-induced
403 pathogenicity, as observed in the lung biopsy specimens.

404 The results generated in the current study increase our understanding of the
405 pathogenesis of pneumonia by demonstrating that the T3SS, and specifically, ExoS and ExoT,
406 disrupt the host response in the lungs. Most importantly, ExoS and ExoT of T3SS induce the
407 activation of NF-κB and AKT, and are able to induce the expression of Muc7, Muc13, Muc15,
408 and Muc19 in the lungs. Although these 4 mucins have not been studied thoroughly yet, they
409 are considered important inflammatory mediators in inflammation of the respiratory tract.
410 Treatment of chronic respiratory inflammation is limited to vaccination against commonly
411 occurring respiratory pathogens, pharmacological bronchodilation, or respiratory infection

412 antibiotics to alleviate dyspnea. Our research results provide a basis for future therapies to
413 prevent and confound lung immunopathology through increasing our understanding of the
414 molecular mechanism of pneumonia.
415
416 **Acknowledgments**
417 This study was supported by the National Research Foundation of Korea (NRF) grant funded
418 by the Ministry of Science, ICT & Future Planning (NRF-2017R1A2B2011555) and awarded
419 to the Korea Research Institute of Bioscience and Biotechnology Research Initiative Program
420 (KGM 1221814) of the Republic of Korea.
421

Figure Captions

Fig 1. Muc7, Muc13, Muc15, and Muc19 expression in PAK-infected A549 and H292 cells. (A–D) PAK MOI- and (E–H) time-dependent increases in Muc7, Muc13, Muc15, and Muc19 mRNA expression as measured by qRT-PCR. Data are presented as the mean ± SD. "–," A549 cells treated with PBS; PAK, A549 cells infected with *P. aeruginosa*. #Significantly different from the normal control group, $*P < 0.05$, $**P < 0.01$, $***P < 0.001$ vs. negative control (PBS) Western blots showing PAK MOI- (I) and time-dependent (J) regulation of Muc7, Muc13, Muc15, and Muc19 protein expression. (K) Intracellular staining of Muc7, Muc13, Muc15, and Muc19 in PAK-infected H292 cells (magnification, 400×). Nuclei were stained with DAPI.

Fig 2. Inhibitory effects of BAY-11-7082 and LY-294002 on the expression of Muc7, Muc13, Muc15, and Muc19 in PAK-infected A549 cells. A549 cells were pretreated with Bay11-7082 or LY-294002 and then infected with PAK (MOI 20) for 4 h. (A–D) Muc7, Muc13, Muc15, and Muc19 mRNA expression as assessed by qRT-PCR. (E) Western blot of Muc7, Muc13, Muc15, and Muc19 protein expression and quantitative data. Western blot bands were quantified using ImageJ software. The data are presented as the mean ± SD. "–," A549 cells treated with PBS; PAK, A549 cells infected with *P. aeruginosa*; Bay, Bay11-7082; LY, LY-294002; #Significantly different from the normal control group, $*P < 0.05$; $**P < 0.01$; $***P < 0.001$, significantly different from the respective controls.

Fig 3. ExsA::Ω affects Muc7, Muc13, Muc15, and Muc19 expression in A549 and H292 cells. The expression levels of Muc7 (A), Muc13 (B), Muc15 (C), and Muc19 (D) mRNA and

445 protein were determined by qRT-PCR and western blotting, respectively. A549 cells were
446 treated with PAK and ExsA::Ω for 1 h, followed by 2 washes for 15 min and further treatment
447 for 4 h. PAK exposure increases the phosphorylation of AKT (E, F) and p65 (H, I) compared
448 with the vehicle control group in A549 cells. Transcription of SP1 (G) and NF-kB (p65) (J)
449 into the nucleus were confirmed by immunocytochemistry (ICC) in H292 cells. The data are
450 presented as the mean ± SD. "–," A549 cells treated with PBS; PAK, A549 cells infected with
451 *P. aeruginosa*; ExsA::Ω, A549 cells infected with ExsA::Ω (no T3SS). #Significantly different
452 from the non-infected control cells, $*P < 0.05$, significantly different from PAK-only-infected
453 cells.
454
455 **Fig 4. ExoS and ExoT are required and each sufficient to induce Muc7, Muc13, Muc15,**
456 **and Muc19 expression in A549 and H292 cells.** (A–D) Muc7, Muc13, Muc15, and Muc19
457 mRNA and protein expression as determined by qRT-PCR and western blotting, respectively.
458 (E–F) The cellular localization of Muc7, Muc13, Muc15, and Muc19 as determined by
459 immunocytochemistry in H292 cells. "–," control A549 and H292 cells treated with PBS only;
460 PAK, A549 or H292 cells infected with *P. aeruginosa*; ExsA::Ω, A549 or H292 cells infected
461 ExsA::Ω (no T3SS); ΔST, PAK-ΔST mutant; Mock, PAKΔSTmt-pUCP18; S, PAKΔSTmt-
462 pUCP18-PAKexoS; T, PAKΔSTmt-pUCP18-PAKexoT (MOI = 200) #Significantly different
463 from the non-infected control cells, $*P < 0.05$, $**P < 0.01$, $***P < 0.001$, significantly different
464 from PAK-only-infected cells.
465
466 **Fig 5. ExoS and ExoT are required and each sufficient to increase NF-κB and AKT**
467 **signaling in A549 cells.** A549 cells were infected with the indicated strains for 1 h. (A) AKT

468 and p-AKT expression as detected by western blotting. Quantification of p-AKT and SP1
469 expression using RAS-4000. (B) A549 cells were transfected with SP1 luciferase (Luc) reporter
470 plasmid (0.1 μg). (C) NF-κB expression as detected by western blotting. Quantification of p-
471 p65 and p-IκB-α expression using RAS-4000. β-actin was used as the internal control. (D)
472 A549 cells were transfected with expression NF-κB luciferase (Luc) reporter plasmid (0.1 μg).
473 At 24 h after transfection, A549 cells were treated with the strains at MOI = 20 for 1 h, and
474 then, luciferase activity was measured. The data were normalized to β-galactosidase activity.
475 All data are representative of 3 independent experiments. Luciferase activities were measured
476 24 h after the transfection. "–," control A549 cells treated with PBS only; PAK, A549 cells
477 infected with *P. aeruginosa*; ExsA::Ω, A549 cells infected with ExsA::Ω (no T3SS); ΔST,
478 PAK-ΔST mutant; Mock, PAKΔSTmt-pUCP18; S, PAKΔSTmt-pUCP18PAKexoS; T,
479 PAKΔSTmt-pUCP18PAKexoT (MOI = 20).
480
481 **Fig 6. ExoS and ExoT are required to induce Muc7, Muc13, Muc15, and Muc19**
482 **expression in lung tissue.** (A–D) Muc7, Muc13, Muc15, and Muc19 mRNA levels as
483 determined by qRT-PCR. (E) Western blot showing Muc7, Muc13, Muc15, and Muc19 protein
484 expression and quantitative data. NC, control mice treated with PBS only; PAK, mice infected
485 with *P. aeruginosa*; ExsA::Ω, mice cells infected ExsA::Ω (no T3SS); ΔST, PAK-ΔST mutant;
486 Mock, PAKΔSTmt-pUCP18; S, PAKΔSTmt-pUCP18PAKexoS; T, PAKΔSTmt-
487 pUCP18PAKexoT (MOI 2.5×10^6) #Significantly different from the non-infected control cells,
488 $*P < 0.05$, $**P < 0.01$, $***P < 0.001$, significantly different from PAK-only-infected cells.
489
490 **Fig 7. ExoS and ExoT are required and each sufficient to increase AKT/SP1 signaling in**

491 **lung tissue.** Western blot showing pAKT, AKT, and SP1 protein expression and quantitative
492 data. NC, control mice treated with PBS only; PAK; ExsA::Ω (no T3SS), ΔST, S, and T (MOI
493 2.5×10^6). #Significantly different from the non-infected control cells, *$P < 0.05$, **$P < 0.01$,
494 significantly different from PAK-only-infected cells.
495
496
497 **Fig 8. Muc7, Muc13, Muc15, Muc19, and proinflammatory cytokine expression require**
498 **the NF-κB pathway activated via IKK-α and IKK-β in A549 cells.** (A–D) qRT-PCR
499 analyses showing Muc7, Muc13, Muc15, and Muc19 mRNA expression upon the addition of
500 siRNAs targeting IKK-α and IKK-β. (E) Western blot showing Muc7, Muc13, Muc15, and
501 Muc19 protein expression upon the addition of siRNAs targeting IKK-α and IKK-β as
502 determined by western blotting and quantitative data. (F–H) Cytokine levels as determined by
503 ELISA. Data are the mean ± SEM of 3 different experiments performed in duplicate.
504
505
506

Supporting information

S1 Fig. Effects of PAK exposure on the phosphorylation of NF-κB and SP1/AKT in A549 cells.

S2 Fig. Effects of inhibitors on the expression of proinflammatory cytokines in PAK infected A549 cells.

S3 Fig. Effects of ExoS and ExoT exposure of proinflammatory cytokines in PAK infected A549 cells.

S4 Fig. Effects of PAK and LPS exposure of the Muc13, Muc15, and Muc19 in mice.

S5 Fig. Histopathology of mouse lungs 20 h after inoculation with *P. aeruginosa* and LPS.

S6 Fig. Muc7, Muc13, Muc15, and Muc19 in A549 after siRNA-mediated downregulation of IKK-α and IKK-β.

S7 Fig. Proinflammatory cytokine in A549 after siRNA-mediated downregulation of IKK-α and IKK-β.

520 **Reference**

521 1. Rangel SM, Diaz MH, Knoten CA, Zhang A, Hauser AR (2015) The Role of ExoS in
522 Dissemination of Pseudomonas aeruginosa during Pneumonia. PLoS Pathog 11:
523 e1004945.
524 2. Collmer A, Badel JL, Charkowski AO, Deng WL, Fouts DE, et al. (2000) Pseudomonas
525 syringae Hrp type III secretion system and effector proteins. Proc Natl Acad Sci U S A
526 97: 8770-8777.
527 3. Ader F, Le Berre R, Faure K, Gosset P, Epaulard O, et al. (2005) Alveolar response to
528 Pseudomonas aeruginosa: role of the type III secretion system. Infect Immun 73: 4263-
529 4271.
530 4. Park JW, Kim YJ, Shin IS, Kwon OK, Hong JM, et al. (2016) Type III Secretion System of
531 Pseudomonas aeruginosa Affects Matrix Metalloproteinase 12 (MMP-12) and MMP-
532 13 Expression via Nuclear Factor kappaB Signaling in Human Carcinoma Epithelial
533 Cells and a Pneumonia Mouse Model. J Infect Dis 214: 962-969.
534 5. Hauser AR (2009) The type III secretion system of Pseudomonas aeruginosa: infection by
535 injection. Nat Rev Microbiol 7: 654-665.
536 6. Engel J, Balachandran P (2009) Role of Pseudomonas aeruginosa type III effectors in disease.
537 Curr Opin Microbiol 12: 61-66.
538 7. Galle M, Jin S, Bogaert P, Haegman M, Vandenabeele P, et al. (2012) The Pseudomonas
539 aeruginosa type III secretion system has an exotoxin S/T/Y independent pathogenic role
540 during acute lung infection. PLoS One 7: e41547.
541 8. Yeung AT, Parayno A, Hancock RE (2012) Mucin promotes rapid surface motility in
542 Pseudomonas aeruginosa. MBio 3.

543 9. Thornton DJ, Carlstedt I, Howard M, Devine PL, Price MR, et al. (1996) Respiratory mucins:
544 identification of core proteins and glycoforms. Biochem J 316 (Pt 3): 967-975.
545 10. Kaliner M, Shelhamer JH, Borson B, Nadel J, Patow C, et al. (1986) Human respiratory
546 mucus. Am Rev Respir Dis 134: 612-621.
547 11. Wickstrom C, Herzberg MC, Beighton D, Svensater G (2009) Proteolytic degradation of
548 human salivary MUC5B by dental biofilms. Microbiology 155: 2866-2872.
549 12. Flynn JM, Niccum D, Dunitz JM, Hunter RC (2016) Evidence and Role for Bacterial Mucin
550 Degradation in Cystic Fibrosis Airway Disease. PLoS Pathog 12: e1005846.
551 13. Porchet N, Dufosse J, Audie JP, Duperat VG, Perini JM, et al. (1991) Structural features of
552 the core proteins of human airway mucins ascertained by cDNA cloning. Am Rev
553 Respir Dis 144: S15-18.
554 14. Dakin CJ, Numa AH, Wang H, Morton JR, Vertzyas CC, et al. (2002) Inflammation,
555 infection, and pulmonary function in infants and young children with cystic fibrosis.
556 Am J Respir Crit Care Med 165: 904-910.
557 15. Cattoir V, Narasimhan G, Skurnik D, Aschard H, Roux D, et al. (2013) Transcriptional
558 response of mucoid Pseudomonas aeruginosa to human respiratory mucus. MBio 3:
559 e00410-00412.
560 16. Canton J, Fehr AR, Fernandez-Delgado R, Gutierrez-Alvarez FJ, Sanchez-Aparicio MT, et
561 al. (2018) MERS-CoV 4b protein interferes with the NF-kappaB-dependent innate
562 immune response during infection. PLoS Pathog 14: e1006838.
563 17. Mei LL, Wang WJ, Qiu YT, Xie XF, Bai J, et al. (2017) miR-145-5p Suppresses Tumor
564 Cell Migration, Invasion and Epithelial to Mesenchymal Transition by Regulating the
565 Sp1/NF-kappaB Signaling Pathway in Esophageal Squamous Cell Carcinoma. Int J

566 Mol Sci 18.
567 18. Yang L, Sun K, Chu J, Qu Y, Zhao X, et al. (2018) Long non-coding RNA FTH1P3
568 regulated metastasis and invasion of esophageal squamous cell carcinoma through
569 SP1/NF-kB pathway. Biomed Pharmacother 106: 1570-1577.
570 19. Kim YJ, Paek SH, Jin S, Park BS, Ha UH (2014) A novel Pseudomonas aeruginosa-derived
571 effector cooperates with flagella to mediate the upregulation of interleukin 8 in human
572 epithelial cells. Microb Pathog 66: 24-28.
573 20. Schultz MJ, Rijneveld AW, Florquin S, Edwards CK, Dinarello CA, et al. (2002) Role of
574 interleukin-1 in the pulmonary immune response during Pseudomonas aeruginosa
575 pneumonia. Am J Physiol Lung Cell Mol Physiol 282: L285-290.
576 21. Tanaka E, Yuba Y, Sato A, Kuze F (1994) Effects of the beige mutation on respiratory tract
577 infection with Pseudomonas aeruginosa in mice. Exp Lung Res 20: 351-366.
578 22. Park JW, Shin IS, Ha UH, Oh SR, Kim JH, et al. (2015) Pathophysiological changes
579 induced by Pseudomonas aeruginosa infection are involved in MMP-12 and MMP-13
580 upregulation in human carcinoma epithelial cells and a pneumonia mouse model. Infect
581 Immun 83: 4791-4799.
582 23. Li R, Tan S, Yu M, Jundt MC, Zhang S, et al. (2015) Annexin A2 Regulates Autophagy in
583 Pseudomonas aeruginosa Infection through the Akt1-mTOR-ULK1/2 Signaling
584 Pathway. J Immunol 195: 3901-3911.
585 24. Song Z, Zhang J, Zhang X, Li D, Wang H, et al. (2015) Interleukin 4 Deficiency Reverses
586 Development of Secondary Pseudomonas aeruginosa Pneumonia During Sepsis-
587 Associated Immunosuppression. J Infect Dis 211: 1616-1627.
588 25. Hacker H, Karin M (2006) Regulation and function of IKK and IKK-related kinases. Sci

589 STKE 2006: re13.
590 26. Liu J, Lu SY, Orfe LH, Ren CH, Hu CQ, et al. (2016) ExsE Is a Negative Regulator for
591 T3SS Gene Expression in Vibrio alginolyticus. Front Cell Infect Microbiol 6: 177.
592 27. Fu H, Coburn J, Collier RJ (1993) The eukaryotic host factor that activates exoenzyme S
593 of Pseudomonas aeruginosa is a member of the 14-3-3 protein family. Proc Natl Acad
594 Sci U S A 90: 2320-2324.
595 28. Maresso AW, Riese MJ, Barbieri JT (2003) Molecular heterogeneity of a type III cytotoxin,
596 Pseudomonas aeruginosa exoenzyme S. Biochemistry 42: 14249-14257.
597 29. Soong G, Parker D, Magargee M, Prince AS (2008) The type III toxins of Pseudomonas
598 aeruginosa disrupt epithelial barrier function. J Bacteriol 190: 2814-2821.
599 30. Barbieri JT, Sun J (2004) Pseudomonas aeruginosa ExoS and ExoT. Rev Physiol Biochem
600 Pharmacol 152: 79-92.
601 31. Sadikot RT, Blackwell TS, Christman JW, Prince AS (2005) Pathogen-host interactions in
602 Pseudomonas aeruginosa pneumonia. Am J Respir Crit Care Med 171: 1209-1223.
603 32. Bouillot S, Munro P, Gallet B, Reboud E, Cretin F, et al. (2017) Pseudomonas aeruginosa
604 Exolysin promotes bacterial growth in lungs, alveolar damage and bacterial
605 dissemination. Sci Rep 7: 2120.
606 33. Saadane A, Soltys J, Berger M (2006) Acute Pseudomonas challenge in cystic fibrosis mice
607 causes prolonged nuclear factor-kappa B activation, cytokine secretion, and persistent
608 lung inflammation. J Allergy Clin Immunol 117: 1163-1169.
609 34. Ramphal R, Houdret N, Koo L, Lamblin G, Roussel P (1989) Differences in adhesion of
610 Pseudomonas aeruginosa to mucin glycopeptides from sputa of patients with cystic
611 fibrosis and chronic bronchitis. Infect Immun 57: 3066-3071.

612 35. Nie YC, Wu H, Li PB, Luo YL, Zhang CC, et al. (2012) Characteristic comparison of three
613 rat models induced by cigarette smoke or combined with LPS: to establish a suitable
614 model for study of airway mucus hypersecretion in chronic obstructive pulmonary
615 disease. Pulm Pharmacol Ther 25: 349-356.
616 36. Liu G, Cooley MA, Nair PM, Donovan C, Hsu AC, et al. (2017) Airway remodelling and
617 inflammation in asthma are dependent on the extracellular matrix protein fibulin-1c. J
618 Pathol 243: 510-523.
619
620

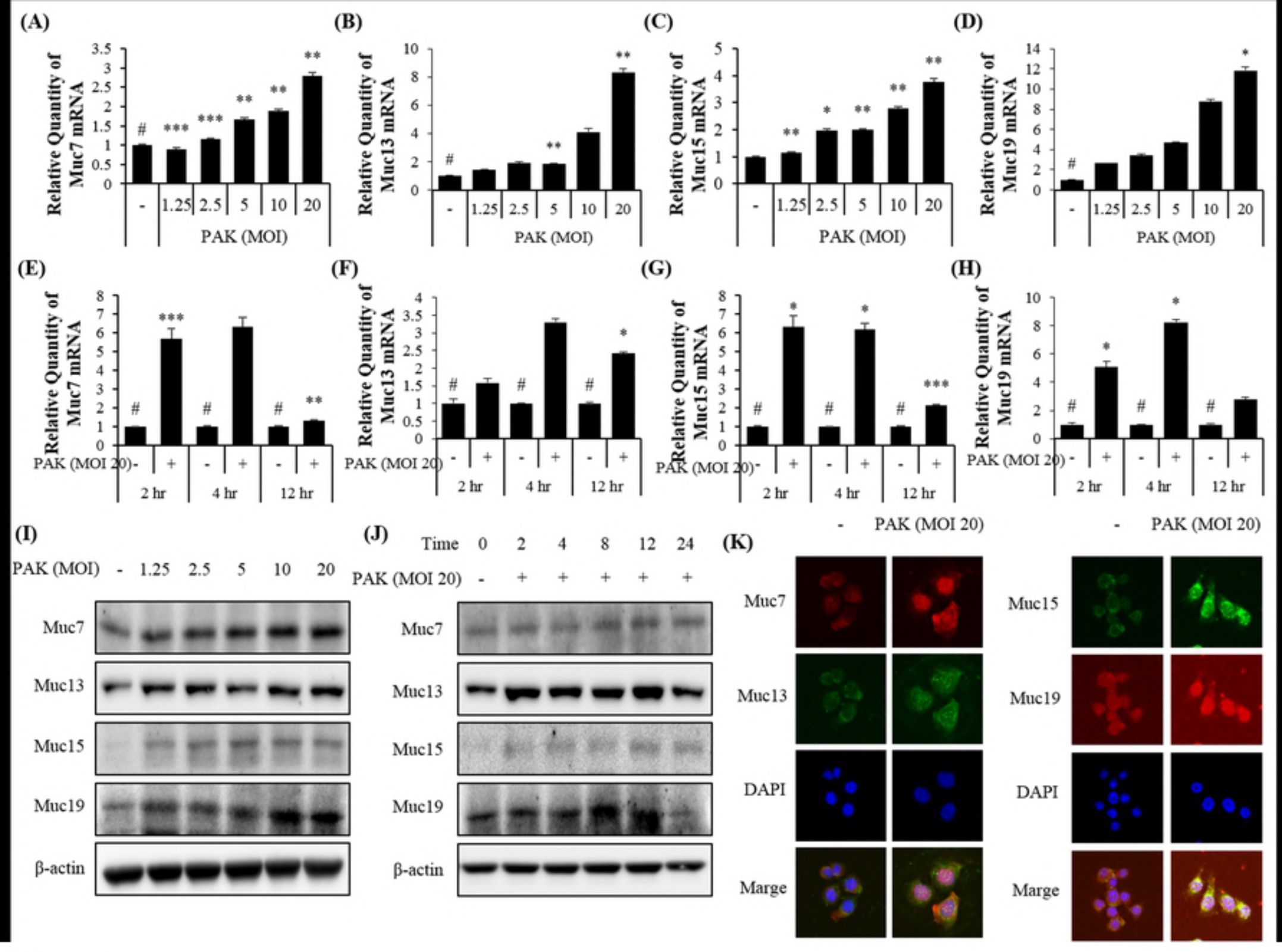
(A)
Relative Quantity of Muc7 mRNA
PAK (MOI)
(B)
Relative Quantity of Muc13 mRNA
PAK (MOI)
(C)
Relative Quantity of Muc15 mRNA
PAK (MOI)
(D)
Relative Quantity of Muc19 mRNA
PAK (MOI)
(E)
Relative Quantity of Muc7 mRNA
PAK (MOI 20)
2 hr
4 hr
12 hr
(F)
Relative Quantity of Muc13 mRNA
PAK (MOI 20)
2 hr
4 hr
12 hr
(G)
Relative Quantity of Muc15 mRNA
PAK (MOI 20)
2 hr
4 hr
12 hr
(H)
Relative Quantity of Muc19 mRNA
PAK (MOI 20)
2 hr
4 hr
12 hr
(I)
PAK (MOI)
Muc7
Muc13
Muc15
Muc19
β-actin
(J)
Time
PAK (MOI 20)
Muc7
Muc13
Muc15
Muc19
β-actin
(K)
PAK (MOI 20)
Muc7
Muc13
DAPI
Marge
PAK (MOI 20)
Muc15
Muc19
DAPI
Marge

Figure

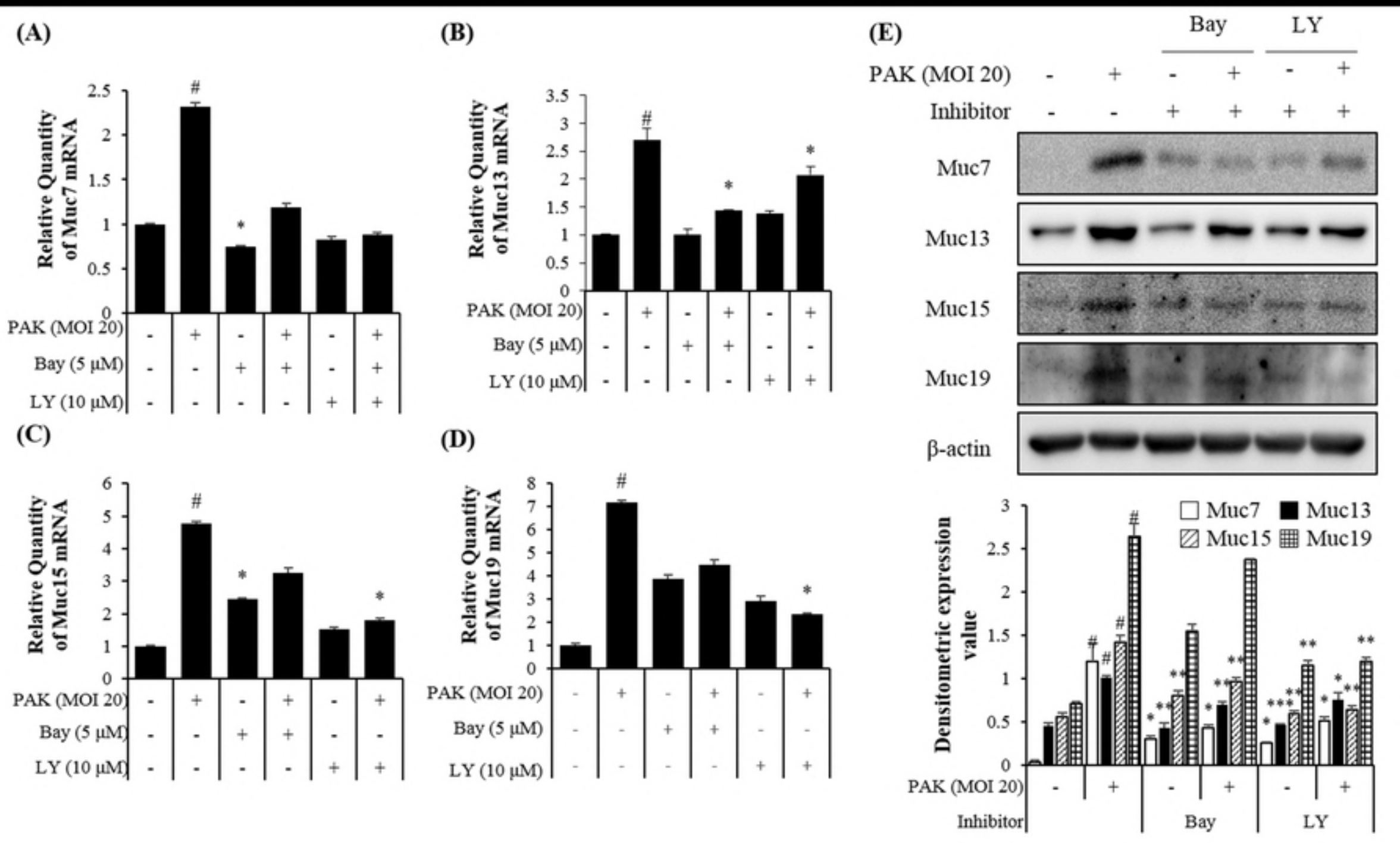
(A)
Relative Quantity of Muc7 mRNA
PAK (MOI 20)
Bay (5 μM)
LY (10 μM)
(B)
Relative Quantity of Muc13 mRNA
PAK (MOI 20)
Bay (5 μM)
LY (10 μM)
(C)
Relative Quantity of Muc15 mRNA
PAK (MOI 20)
Bay (5 μM)
LY (10 μM)
(D)
Relative Quantity of Muc19 mRNA
PAK (MOI 20)
Bay (5 μM)
LY (10 μM)
(E)
Bay
LY
PAK (MOI 20)
Inhibitor
Muc7
Muc13
Muc15
Muc19
β-actin
Densitometric expression value
Muc7
Muc13
Muc15
Muc19
PAK (MOI 20)
Inhibitor
Bay
LY

Figure

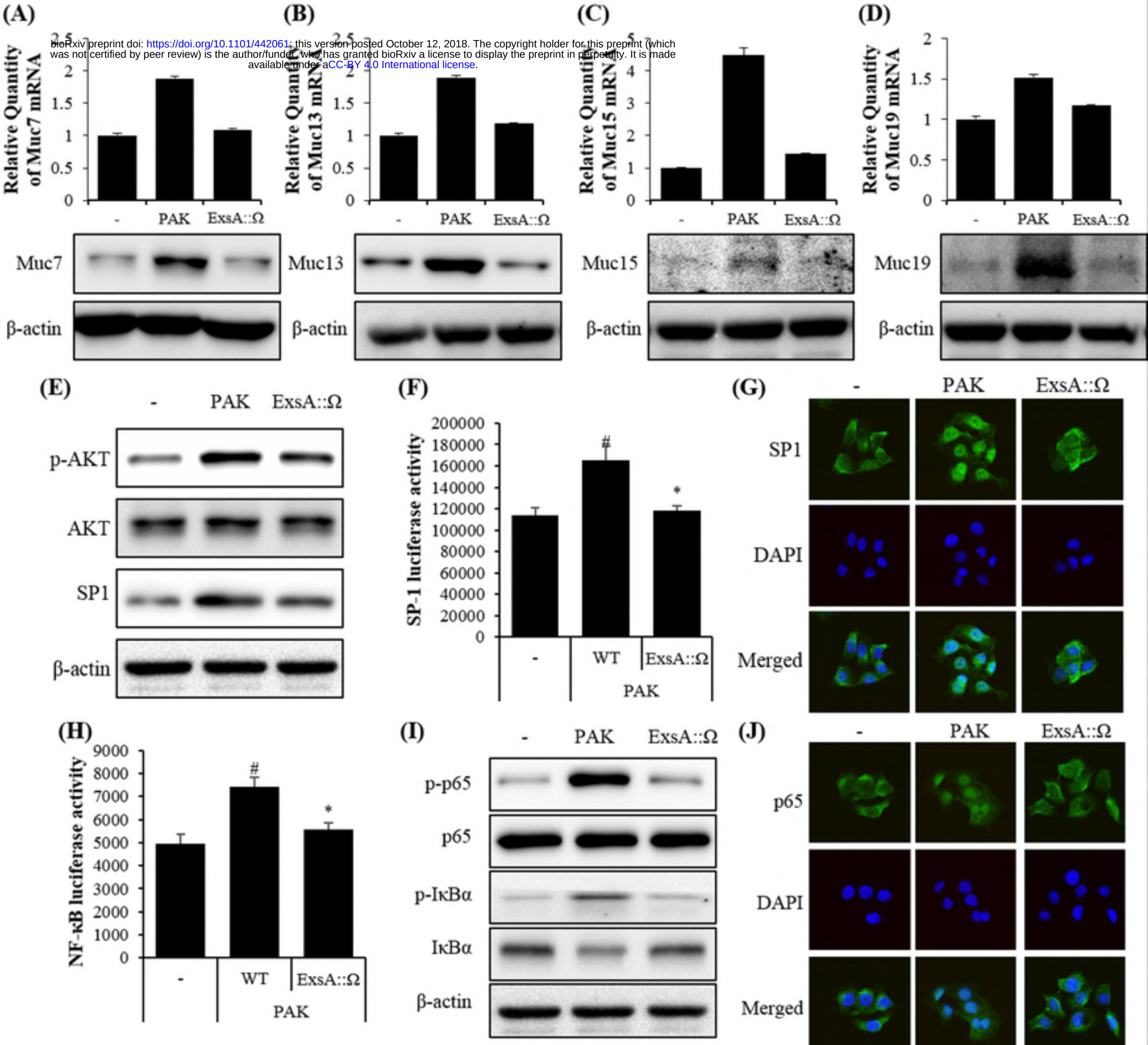

Figure

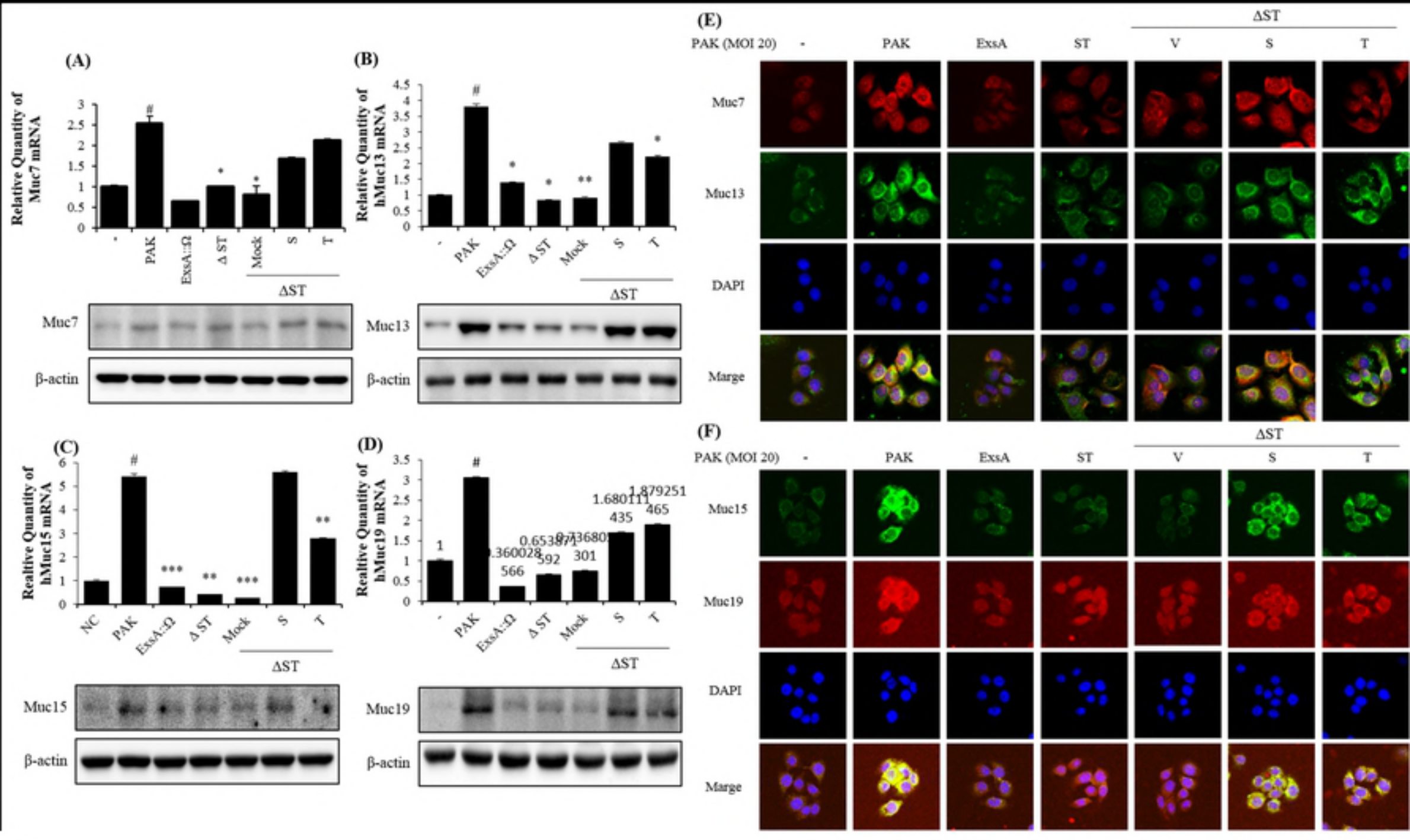
(A)
Relative Quantity of Muc7 mRNA
PAK
ExsA::Ω
Δ ST
Mock
S
T
ΔST
Muc7
β-actin
(B)
Relative Quantity of hMuc13 mRNA
Muc13
(C)
Realtive Quantity of hMuc15 mRNA
NC
Muc15
(D)
Realtive Quantity of hMuc19 mRNA
1
566
592
301
435
465
1.680111
1.879251
Muc19
(E)
PAK (MOI 20)
ExsA
ST
V
Muc7
Muc13
DAPI
Marge
(F)
Muc15
Muc19

Figure

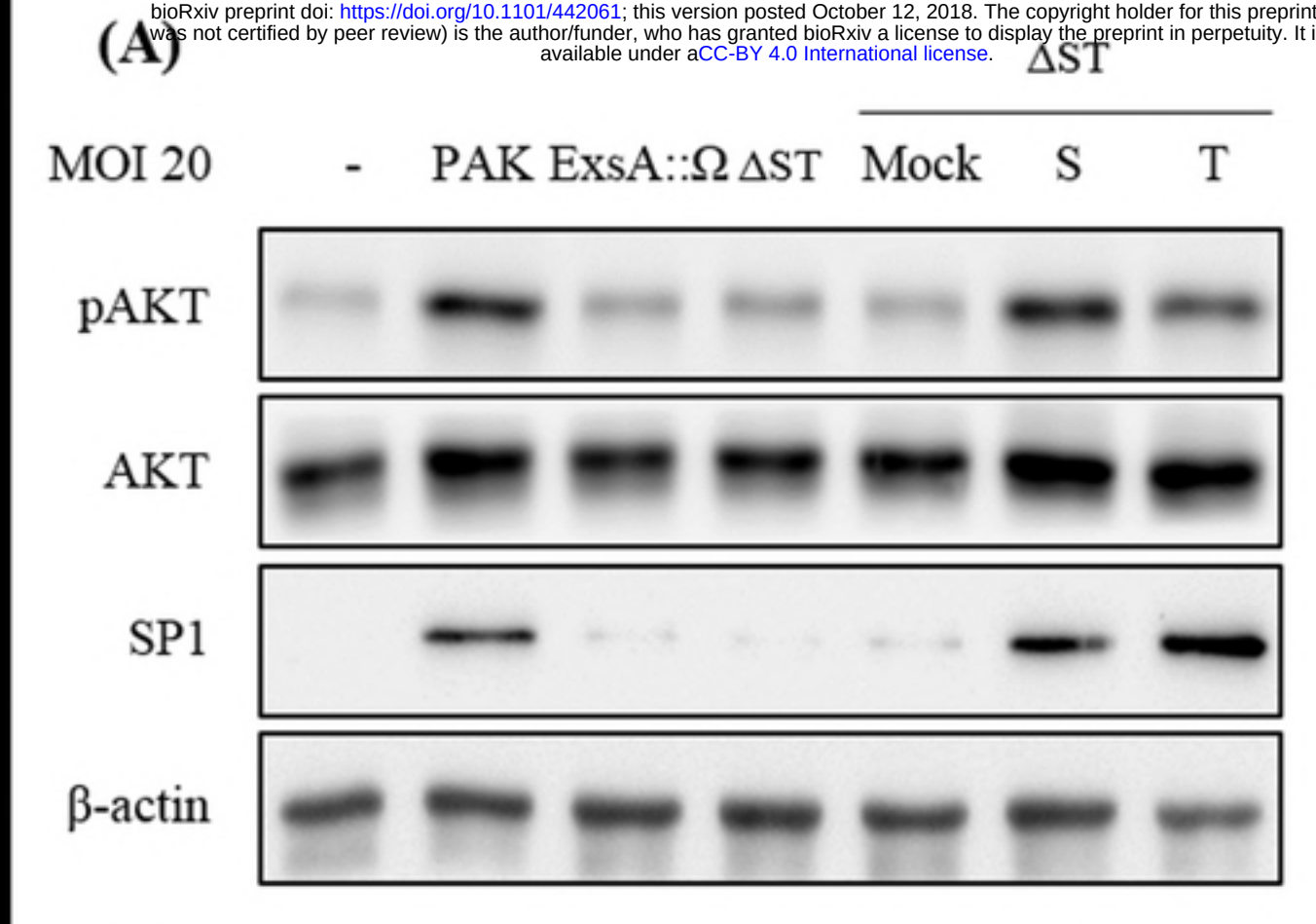

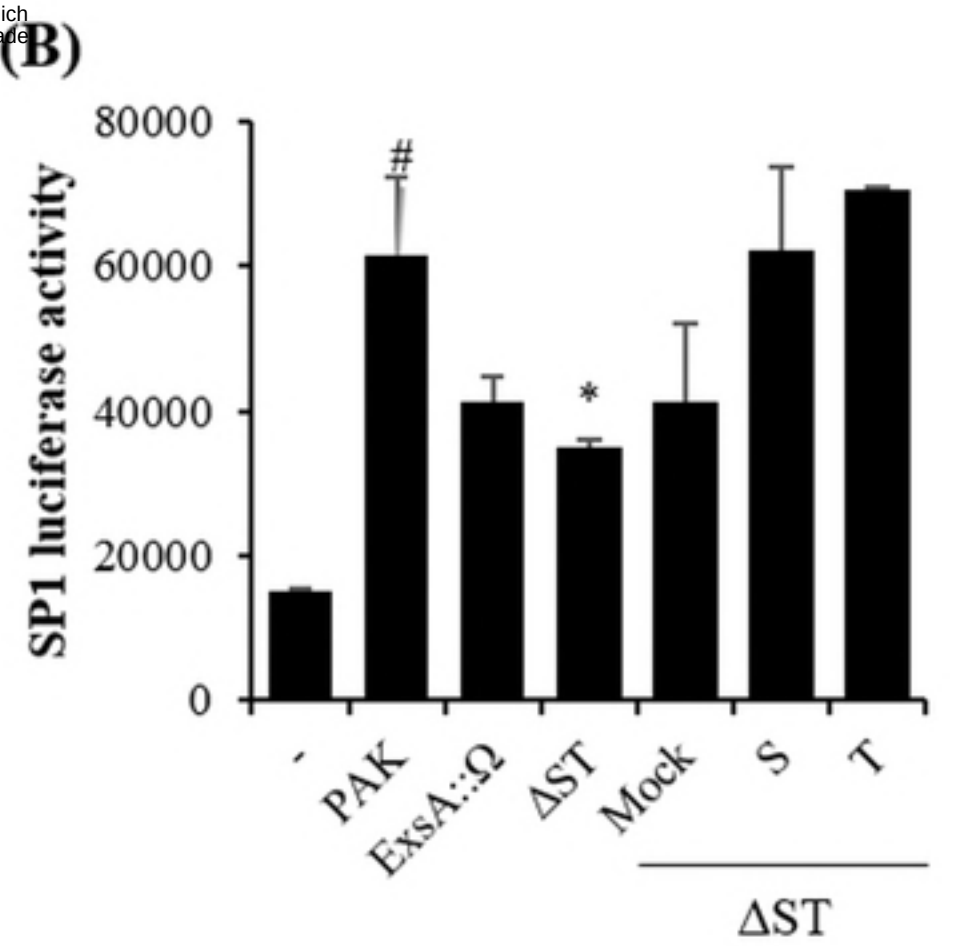

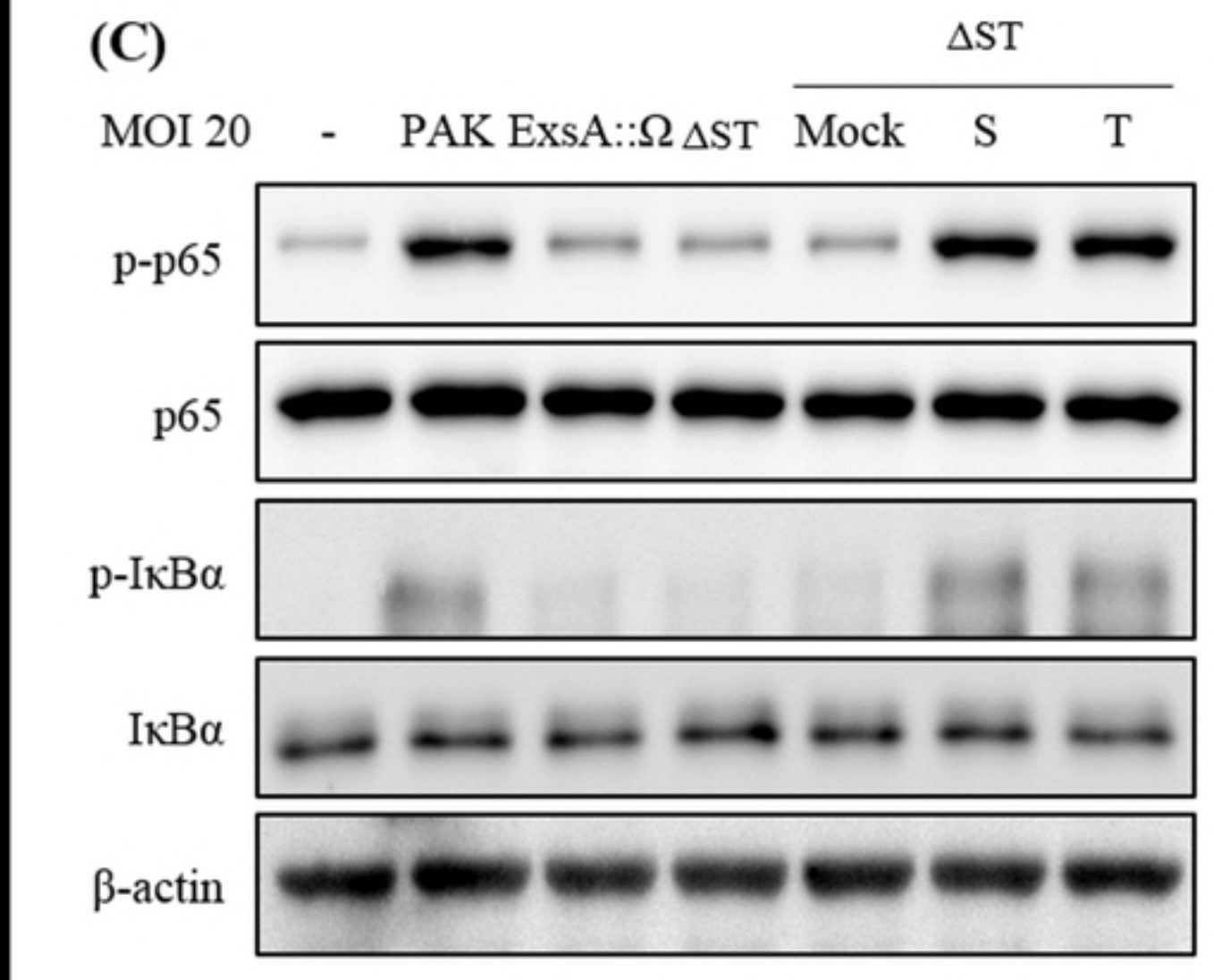

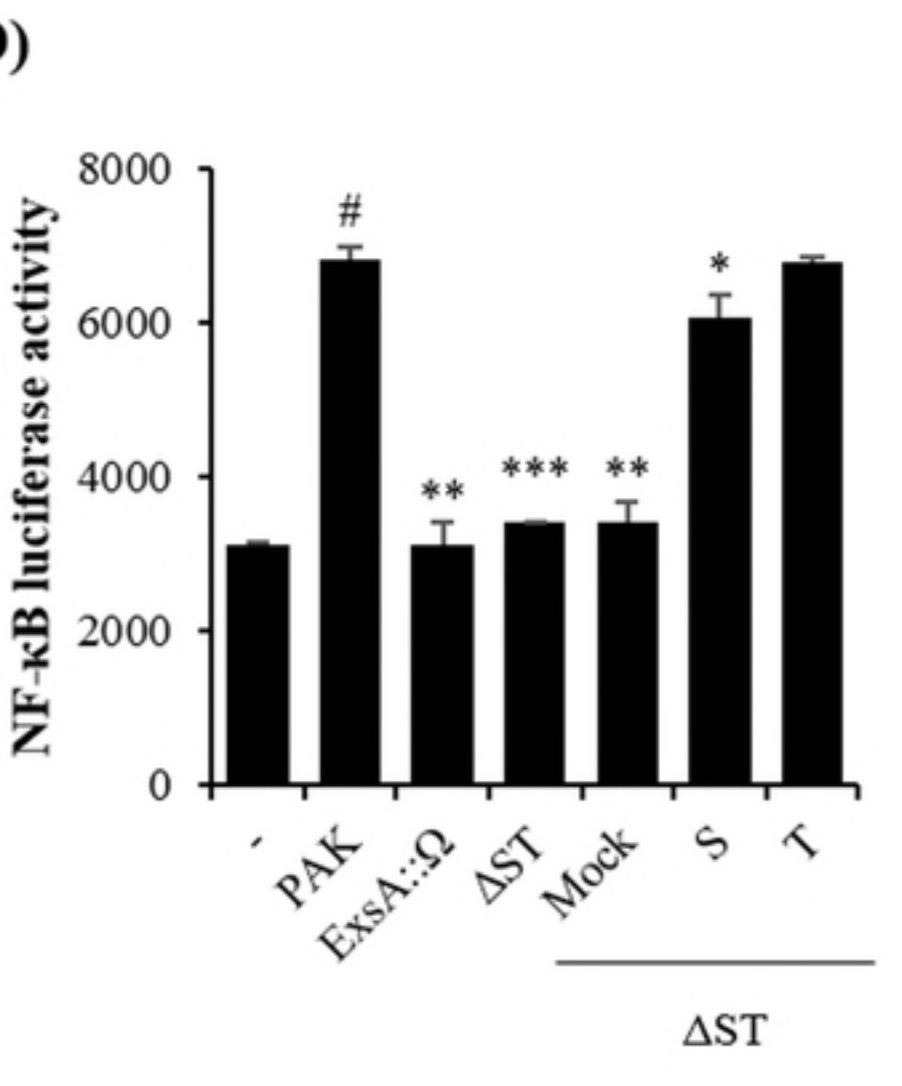

Figure

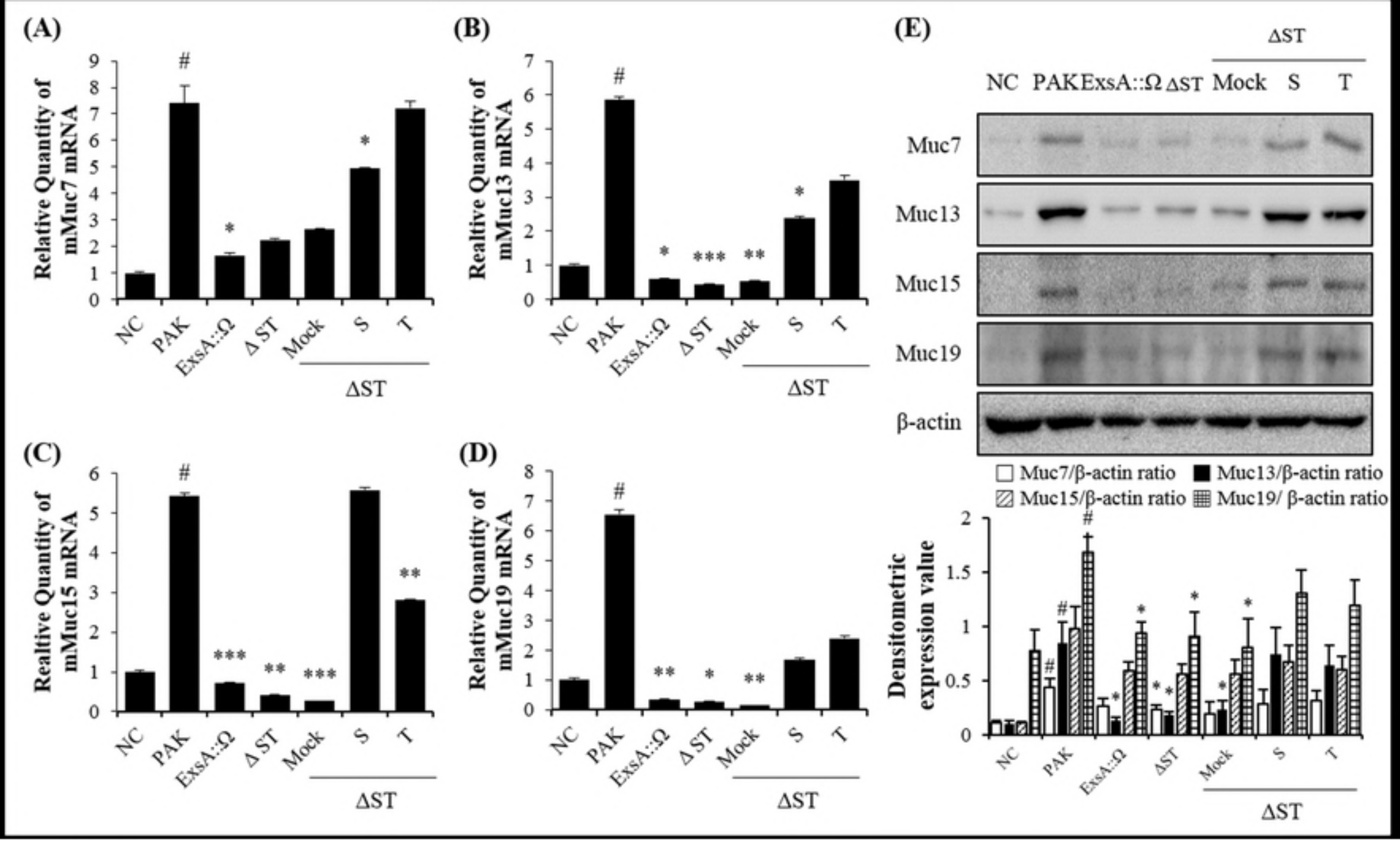
(A)
Relative Quantity of mMuc7 mRNA
NC
PAK
ExsA::Ω
Δ ST
Mock
S
T
ΔST
(B)
Realtive Quantity of mMuc13 mRNA
(C)
Realtive Quantity of mMuc15 mRNA
(D)
Relative Quantity of mMuc19 mRNA
(E)
ΔST
NC PAK ExsA::Ω ΔST Mock S T
Muc7
Muc13
Muc15
Muc19
β-actin
Muc7/β-actin ratio
Muc13/β-actin ratio
Muc15/β-actin ratio
Muc19/ β-actin ratio
Densitometric expression value

Figure

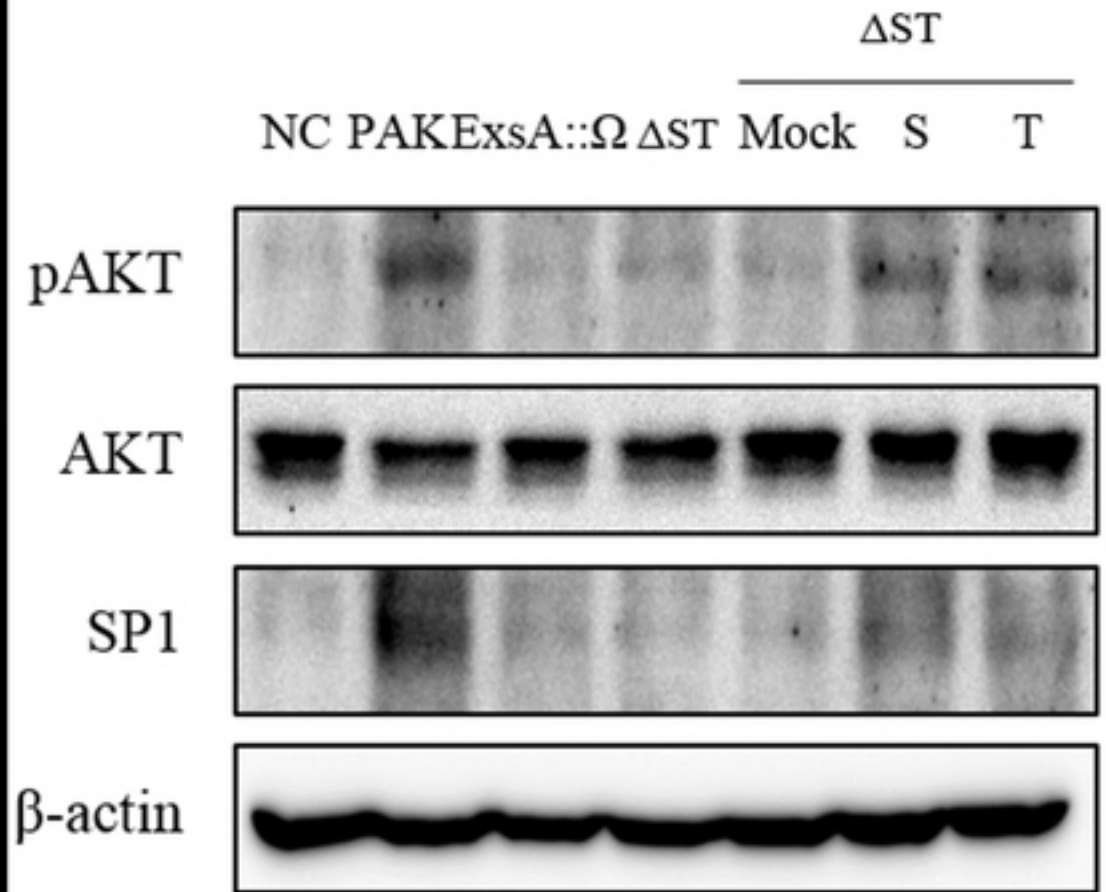
ΔST
NC PAK ExsA::Ω ΔST Mock S T
pAKT
AKT
SP1
β-actin

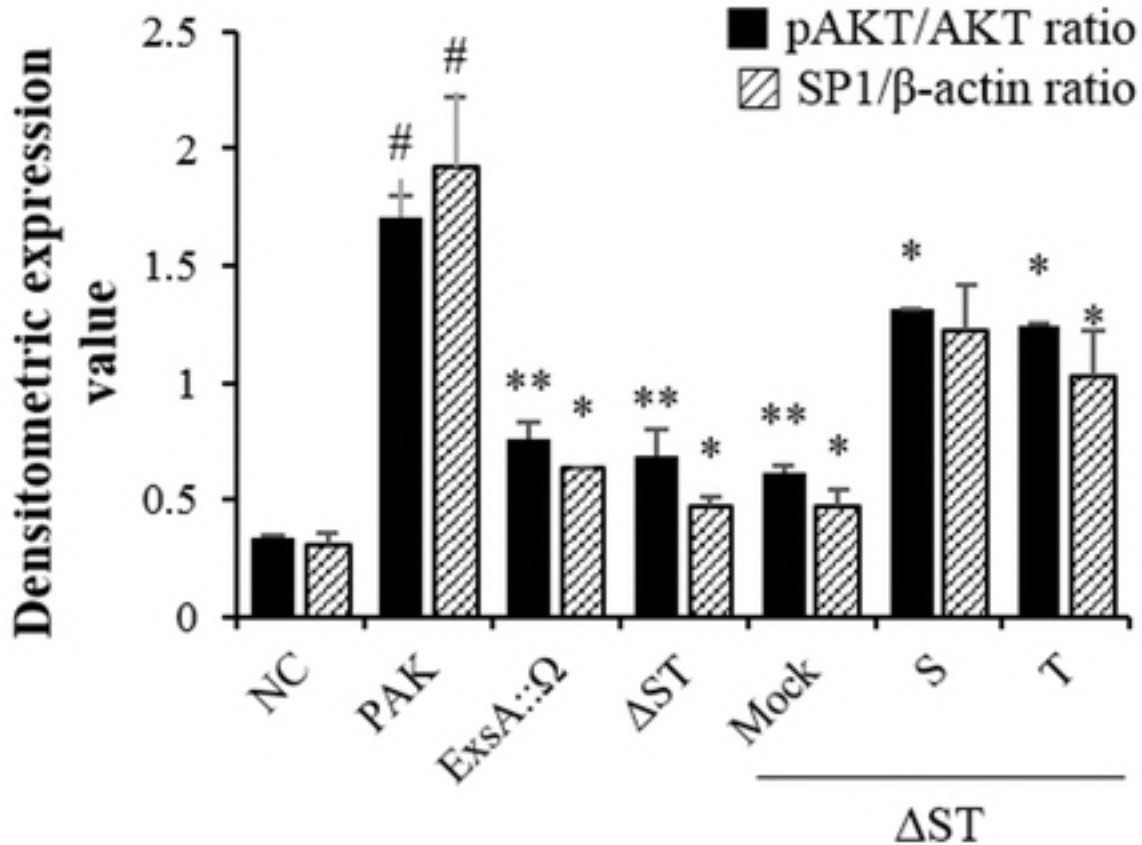
pAKT/AKT ratio
SP1/β-actin ratio
Densitometric expression value
2.5
2
1.5
1
0.5
0
NC
PAK
ExsA::Ω
ΔST
Mock
S
T
ΔST

Figure

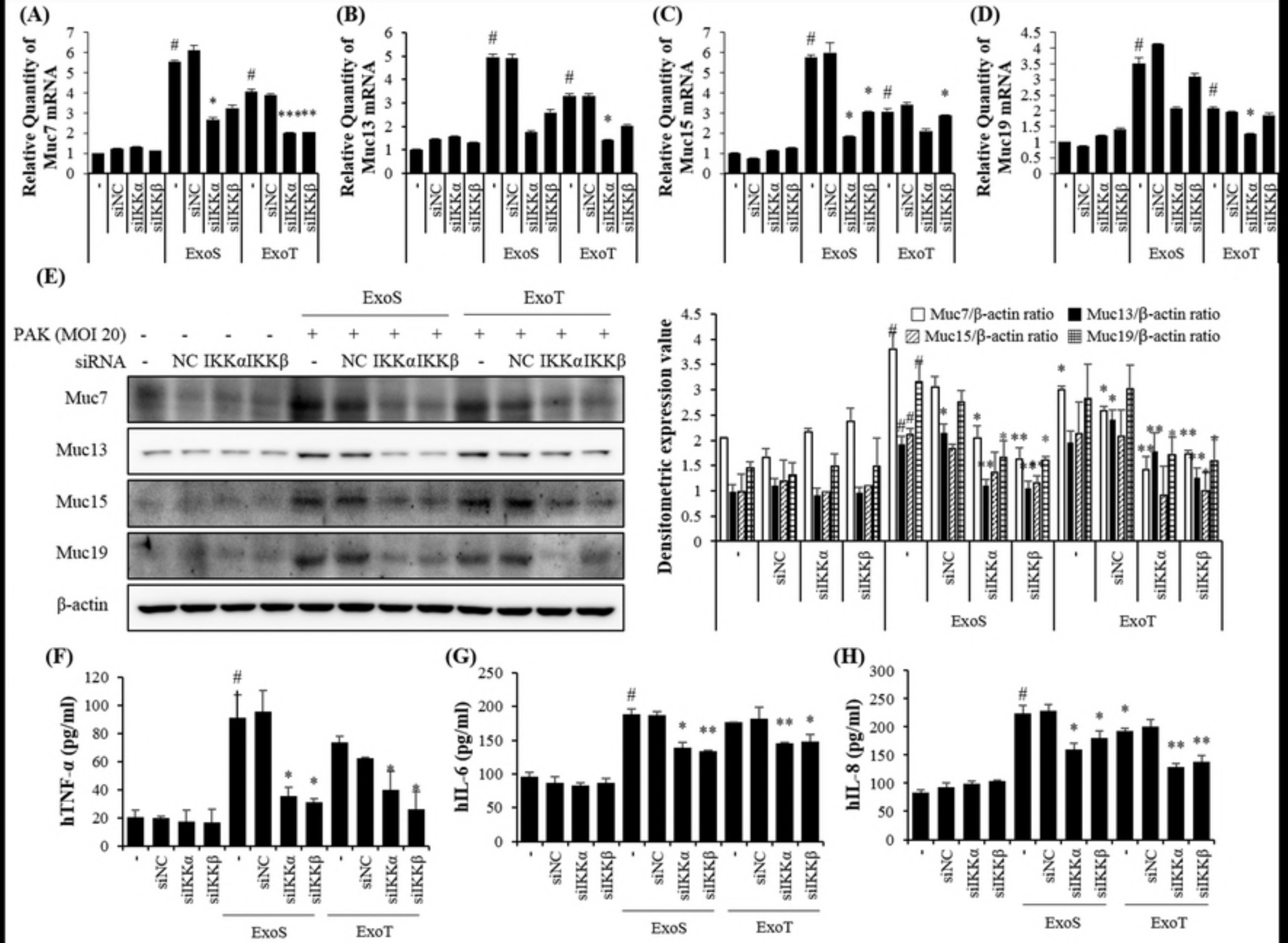
(A)
Relative Quantity of Muc7 mRNA
(B)
Relative Quantity of Muc13 mRNA
(C)
Relative Quantity of Muc15 mRNA
(D)
Relative Quantity of Muc19 mRNA
-
siNC
siIKKα
siIKKβ
ExoS
ExoT
(E)
PAK (MOI 20)
siRNA
NC IKKα IKKβ
Muc7
Muc13
Muc15
Muc19
β-actin
Densitometric expression value
Muc7/β-actin ratio
Muc13/β-actin ratio
Muc15/β-actin ratio
Muc19/β-actin ratio
(F)
hTNF-α (pg/ml)
(G)
hIL-6 (pg/ml)
(H)
hIL-8 (pg/ml)

Figure

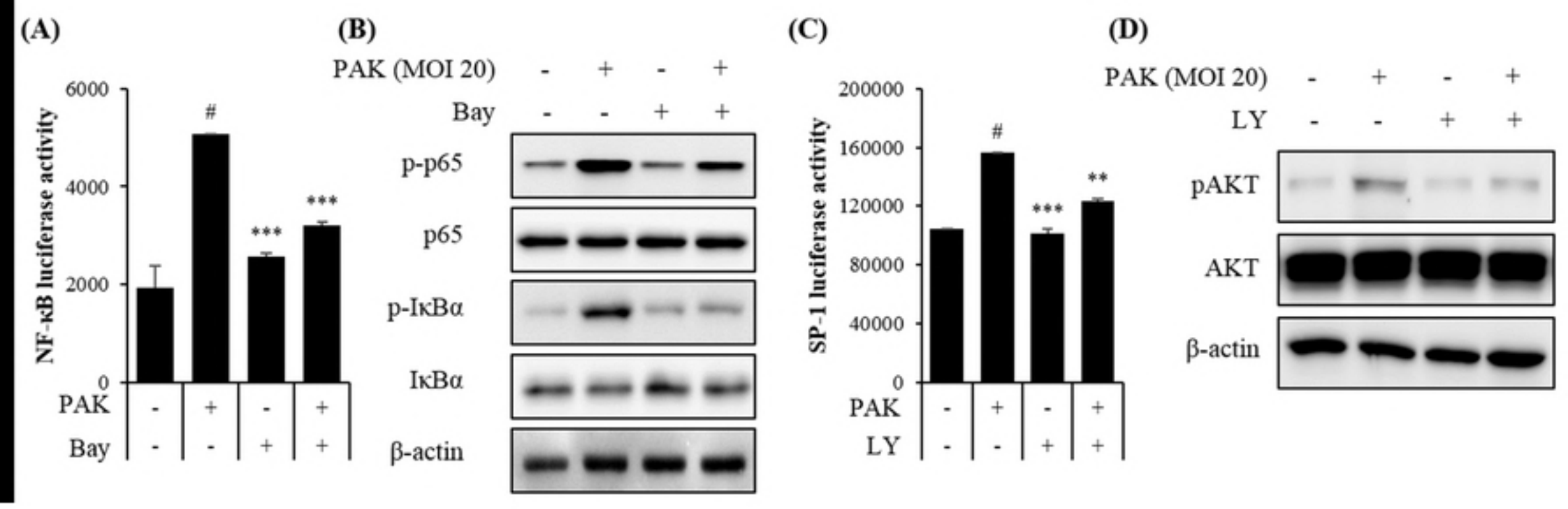
(A)
NF-κB luciferase activity
6000
4000
2000
0
#
***
***
PAK
Bay
(B)
PAK (MOI 20)
Bay
p-p65
p65
p-IκBα
IκBα
β-actin
(C)
SP-1 luciferase activity
200000
160000
120000
80000
40000
0
#
***
**
PAK
LY
(D)
PAK (MOI 20)
LY
pAKT
AKT
β-actin

Figure

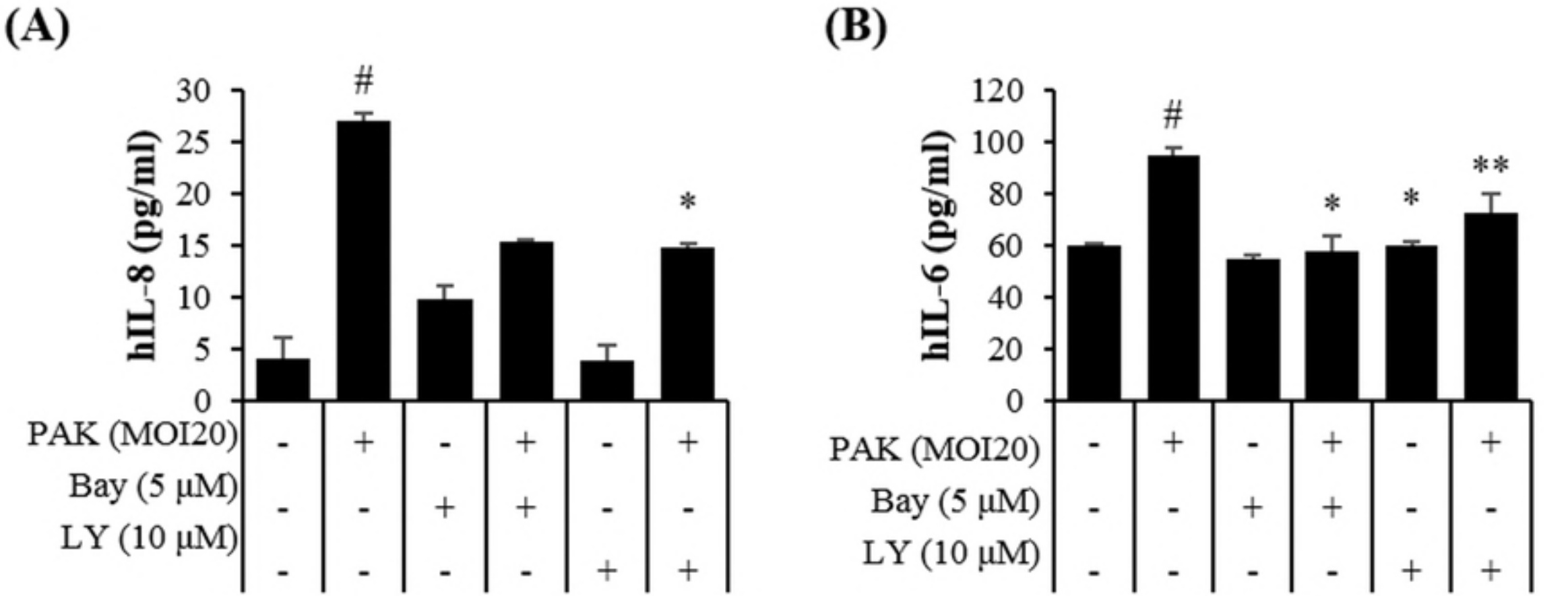
(A)
hIL-8 (pg/ml)
30
25
20
15
10
5
0
#
*
PAK (MOI20) - + - + - +
Bay (5 μM) - - + + - -
LY (10 μM) - - - - + +
(B)
hIL-6 (pg/ml)
120
100
80
60
40
20
0
#
*
*
**
PAK (MOI20) - + - + - +
Bay (5 μM) - - + + - -
LY (10 μM) - - - - + +
(C)
Relative Quantity of IL-8 mRNA
9
8
7
6
5
4
3
2
1
0
#
**
*
*
PAK (MOI 20) - + - + - +
Bay (5 μM) - - + + - -
LY (10 μM) - - - - + +
(D)
Relative Quantity of IL-6 mRNA
40
35
30
25
20
15
10
5
0
#
*
PAK (MOI 20) - + - + - +
Bay (5 μM) - - + + - -
LY (10 μM) - - - - + +

Figure

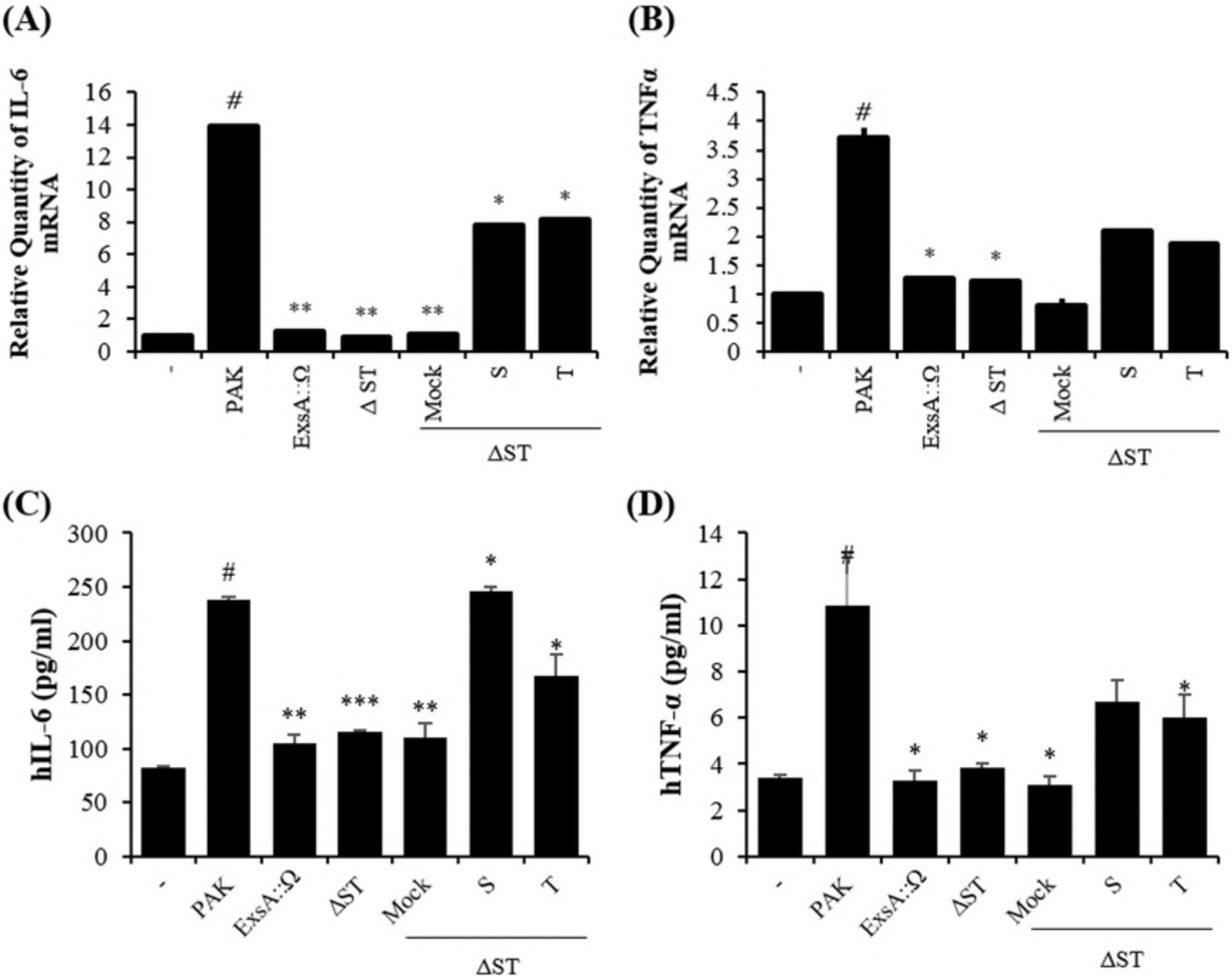
(A)
Relative Quantity of IL-6 mRNA
16
14
12
10
8
6
4
2
0
#
**
**
**
*
*
-
PAK
ExsA::Ω
Δ ST
Mock
S
T
ΔST
(B)
Relative Quantity of TNFα mRNA
4.5
4
3.5
3
2.5
2
1.5
1
0.5
0
#
*
*
-
PAK
ExsA::Ω
Δ ST
Mock
S
T
ΔST
(C)
hIL-6 (pg/ml)
300
250
200
150
100
50
0
#
**
***
**
*
*
-
PAK
ExsA::Ω
ΔST
Mock
S
T
ΔST
(D)
hTNF-α (pg/ml)
14
12
10
8
6
4
2
0
#
*
*
*
-
PAK
ExsA::Ω
ΔST
Mock
S
T
ΔST

Figure

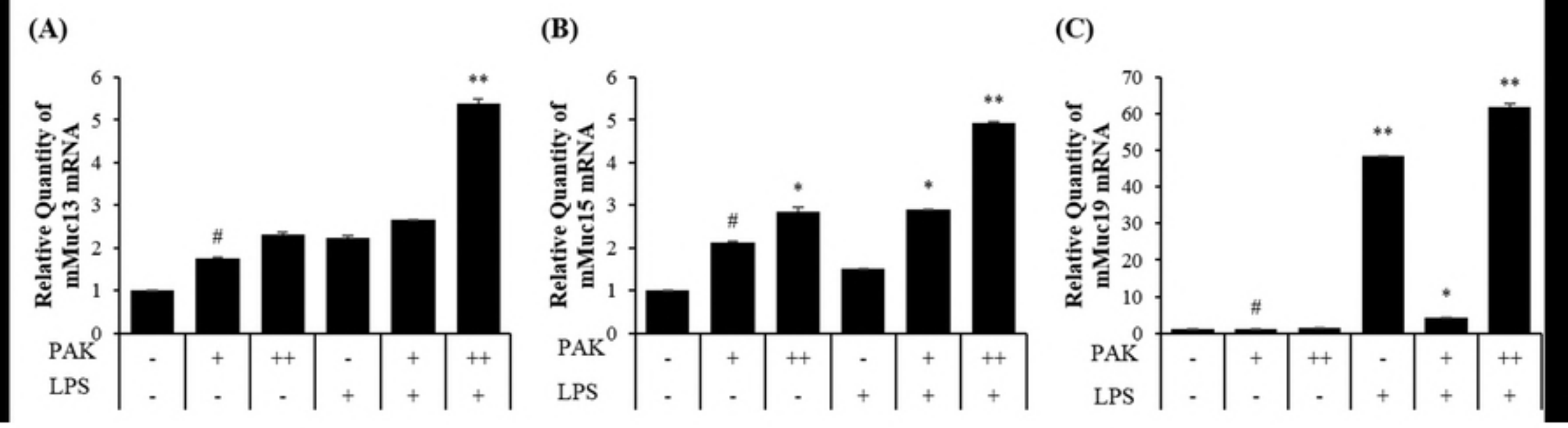
(A)
Relative Quantity of mMuc13 mRNA
6
5
4
3
2
1
0
#
**
PAK
LPS
-
+
++
-
+
++
-
-
-
+
+
+
(B)
Relative Quantity of mMuc15 mRNA
6
5
4
3
2
1
0
#
*
*
**
PAK
LPS
-
+
++
-
+
++
-
-
-
+
+
+
(C)
Relative Quantity of mMuc19 mRNA
70
60
50
40
30
20
10
0
#
**
*
**
PAK
LPS
-
+
++
-
+
++
-
-
-
+
+
+

Figure

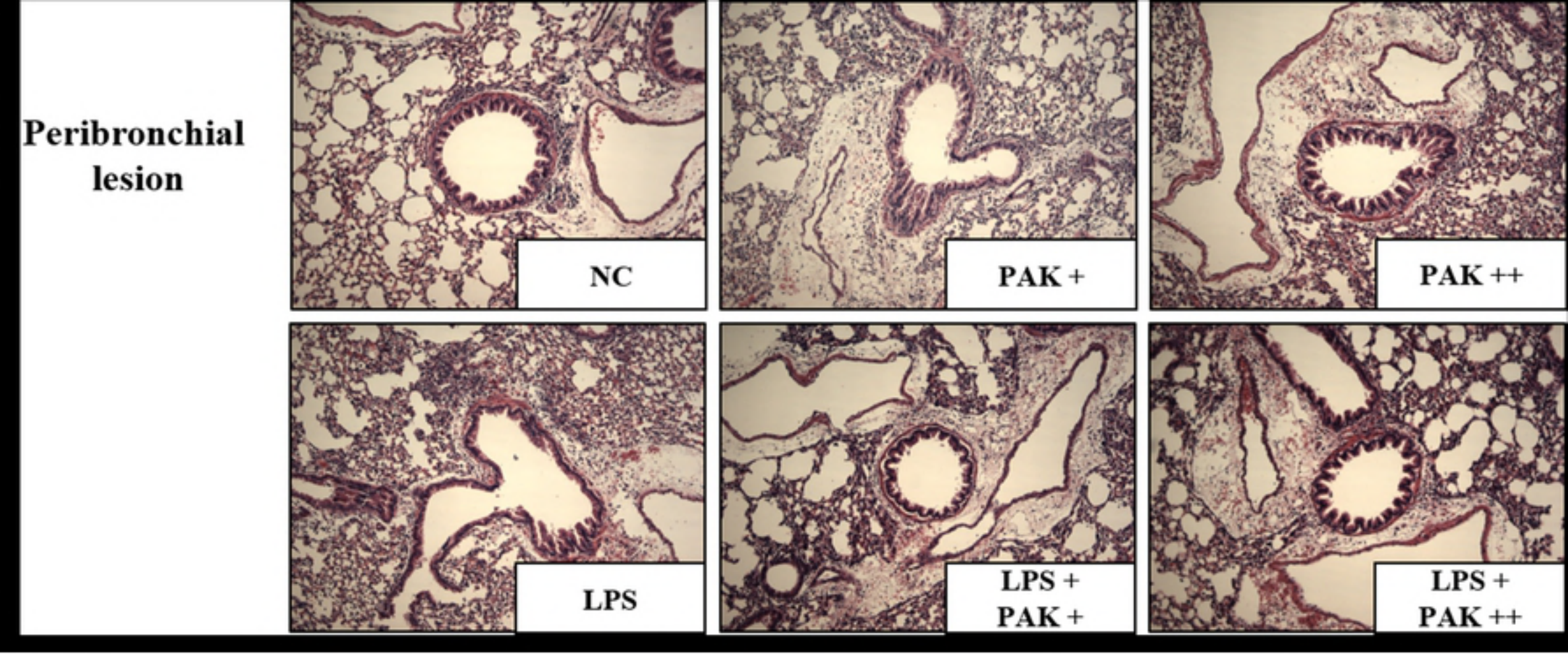

Figure

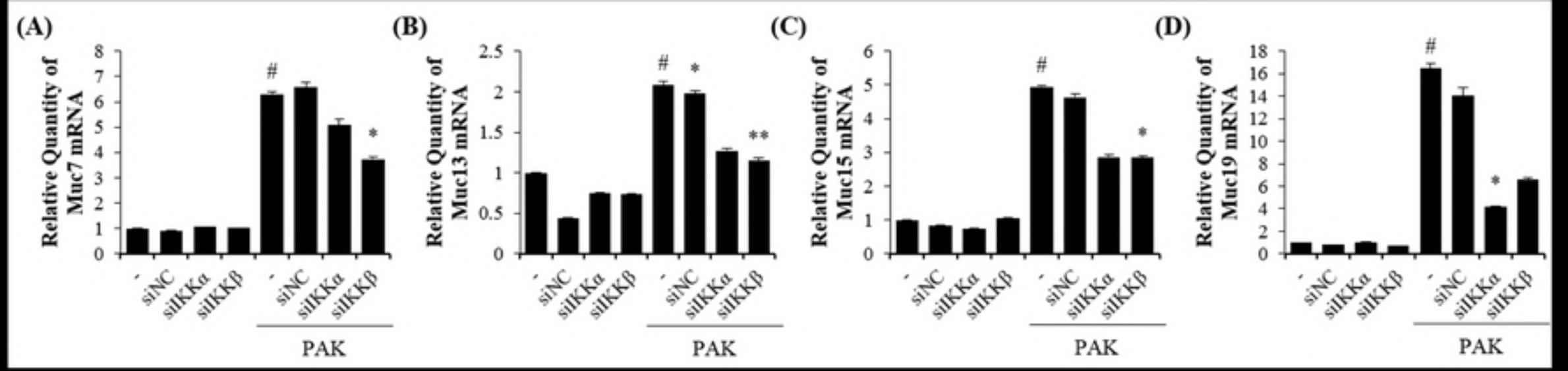
(A)
Relative Quantity of Muc7 mRNA
(B)
Relative Quantity of Muc13 mRNA
(C)
Relative Quantity of Muc15 mRNA
(D)
Relative Quantity of Muc19 mRNA
-
siNC
siIKKα
siIKKβ
PAK

Figure

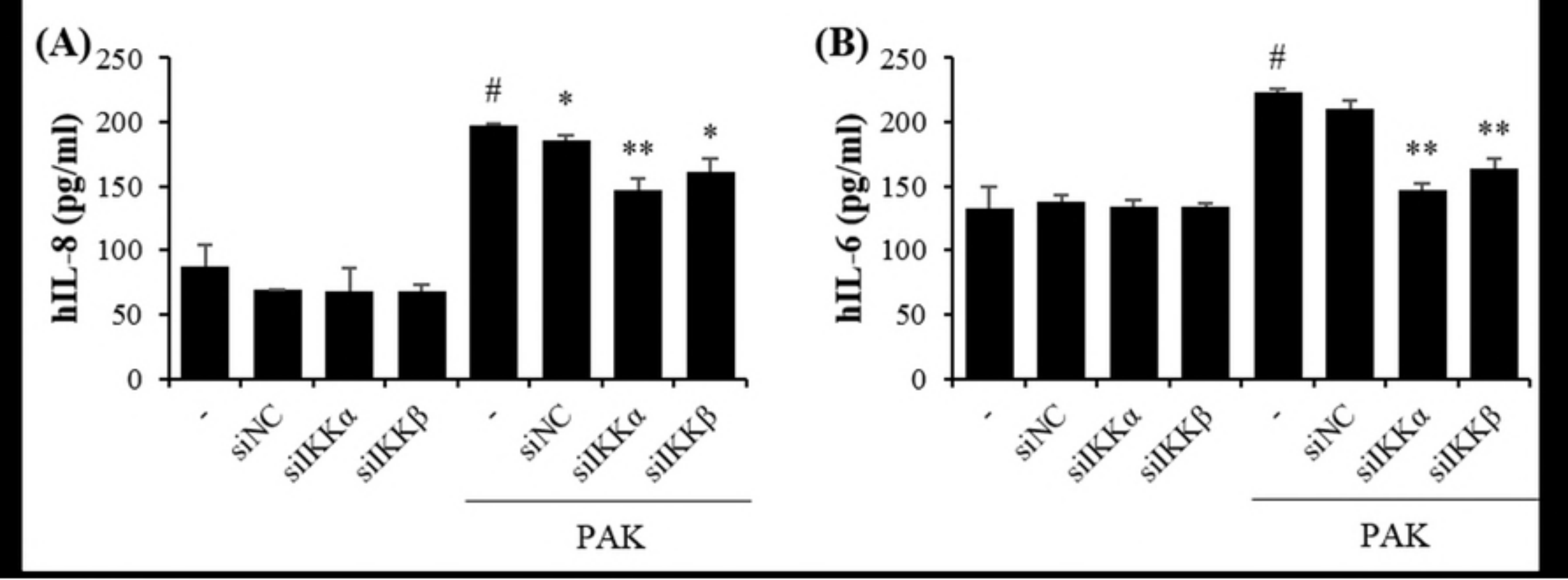
(A)
hIL-8 (pg/ml)
250
200
150
100
50
0
#
*
**
*
-
siNC
siIKKα
siIKKβ
-
siNC
siIKKα
siIKKβ
PAK
(B)
hIL-6 (pg/ml)
250
200
150
100
50
0
#
**
**
-
siNC
siIKKα
siIKKβ
-
siNC
siIKKα
siIKKβ
PAK

Figure